



VILNIAUS UNIVERSITETAS
FACULTY OF MATHEMATICS AND INFORMATICS
(MASTER IN MATHEMATICS)

(MASTER THESIS)

Study of a single dynamical system
Vienos dinaminės sistemos tyrimas

Osama Ahmad

Supervisor : Dr. Audrius Kačėnas

Reviewer : Dr. Artūras Štikonas

Vilnius
2025

Acknowledgements

First and foremost, I would like to express my deepest gratitude to my supervisor, Dr. Audrius Kačėnas, for their unwavering guidance, constructive feedback, and invaluable support throughout the development of this thesis. Their expertise and encouragement have been instrumental in shaping both the direction and quality of my research. I am also grateful to the faculty and staff of Mathematics Department, Vilnius University, for providing a stimulating academic environment and for their commitment to excellence in education and research. Special thanks to my professors whose insightful lectures and discussions inspired much of my interest in dynamical systems and mathematical theory. I sincerely thank my fellow students and friends for their camaraderie, encouragement, and the many moments of laughter and shared challenges. Your support made this journey not only intellectually enriching but also personally meaningful. To my family, I owe heartfelt thanks. Your constant love, patience, and belief in my abilities have been a source of strength throughout this academic journey. Without your sacrifices and support, none of this would have been possible.

Santrauka

Šiame darbe nagrinėjamas vienmatės dinaminės sistemos $([0, 1], \mathcal{B}, m, \mathcal{S})$ matų teorinis elgesys, kur sistema apibrėžiama žemėlapiu $\mathcal{S}(\xi) = \{\rho\xi\}$, kai $\rho > 1$ yra iracionalusis skaičius, o $\{\cdot\}$ žymi trupmeninę dalį. Tyrime nagrinėjami trys konkretūs atvejai: $\mathcal{S}_1(\xi) = \{G\xi\}$, kur $G = \frac{1+\sqrt{5}}{2}$ (auksinis pjūvis); $\mathcal{S}_2(\xi) = \{\rho_2\xi\}$, kai $\rho_2 = \frac{1+\sqrt{3}}{2}$; ir $\mathcal{S}_3(\xi) = \{\rho_3\xi\}$, kai $\rho_3 = \frac{1+\sqrt{7}}{2}$. Kiekvienai transformacijai aiškiai išvedamas atitinkamas Perrono operatorius, kuris dėl netolydumo taške $\xi = \frac{1}{\rho}$ turi dalinai apibrėžtą struktūrą. Analitiškai parodyta, kad nė viena iš šių transformacijų neišlaiko Lebegeo mato. Auksinio pjūvio atveju žinoma dalimis pastovi invariantinė tankio funkcija yra pakartotinai pateikiama ir patvirtinama. Tuo tarpu ρ_2 ir ρ_3 atvejais analitinė invariantinių tankių išvestis pasirodė esanti nepraktiška, todėl buvo taikyti skaitiniai vertinimo metodai. Naudojant ilgų orbitų simuliacijas (20000 iteracijų) sugeneruotos empirinės dažnio histogramų aproksimacijos parodė šių žemėlapių invariantinius tankius ir atskleidė jų netolygų statistinį pasiskirstymą. Rezultatai rodo, kad net ir paprastos linijinės transformacijos su iracionaliu masteliu gali turėti sudėtingą invariantinį elgesį, o mato išsaugojimas nėra garantuotas vien tik dėl linijiškumo ar iracionalumo. Perrono operatoriaus teorija veiksmingai aprašo masės perskirstymą laike ir pabrėžia transformacijos netolydumo taško įtaką invariantinėms priemonėms.

Raktažodžiai: Dinaminės sistemos, Perrono operatorius, Lebegeo matas, Invariantinis tankis

Abstract

This thesis investigates the measure-theoretic behavior of a one-dimensional dynamical system $([0, 1), \mathcal{B}, m, \mathcal{S})$, defined by the map $\mathcal{S}(\xi) = \{\rho\xi\}$, where $\rho > 1$ is an irrational number and $\{\cdot\}$ denotes the fractional part. The study focuses on three specific cases: $\mathcal{S}_1(\xi) = \{G\xi\}$, with $G = \frac{1+\sqrt{5}}{2}$ (the golden ratio); $\mathcal{S}_2(\xi) = \{\rho_2\xi\}$, with $\rho_2 = \frac{1+\sqrt{3}}{2}$; and $\mathcal{S}_3(\xi) = \{\rho_3\xi\}$, with $\rho_3 = \frac{1+\sqrt{7}}{2}$. For each transformation, the associated Perron operator is derived explicitly, revealing a piecewise structure due to a discontinuity at $\xi = \frac{1}{\rho}$. It is shown analytically that the Lebesgue measure is not invariant under any of these maps. For the golden ratio map, a known piecewise constant invariant density is revisited and verified. In the cases of ρ_2 and ρ_3 , analytical derivation of invariant densities proved intractable, and instead, numerical estimation was employed. Empirical frequency histograms generated from long orbit simulations (20000 iterations) provided approximate invariant densities for these maps, capturing their non-uniform statistical structure. The results demonstrate that even simple linear transformations with irrational scaling can exhibit complex invariant behavior, and that measure preservation is not implied by linearity or irrationality alone. The Perron framework effectively captures the redistribution of mass over time and highlights the structural influence of the map's discontinuity on invariant measures.

Keywords: Dynamical Systems, Perron Operator, Lebesgue Measure, Invariant Density

Contents

Contents	4
List of Figures	6
List of Tables	7
1 Introduction	9
2 Literature Review	11
2.1 Problem Statement	12
2.2 Research Objectives	12
2.3 Thesis Outline	13
3 Preliminary Notion	15
3.1 Measures and Measure Spaces	15
3.1.1 Perron Operator	16
3.2 Invariant Measures and Measure-Preserving Transformations	18
4 Study of a single dynamical system	22
4.1 Analysis of $\mathcal{S}_1(\xi) = \{G\xi\}$	22
4.1.1 Trajectory under $\mathcal{S}_1(\xi) = \{G\xi\}$	22
4.1.2 Perron Operator for $\mathcal{S}_1(\xi) = \{G\xi\}$	24
4.1.3 Is the Lebesgue Measure Invariant?	26
4.1.4 Invariant Density of $\mathcal{S}_1(\xi)$	27
4.1.5 Frequency Analysis of $\mathcal{S}_1(\xi) = \{G\xi\}$	29
4.2 Analysis of $\mathcal{S}_2(\xi) = \{\rho\xi\}$	31
4.2.1 Trajectory under $\mathcal{S}_2(\xi) = \{\rho\xi\}$	31
4.2.2 Perron Operator for $\mathcal{S}_2(\xi) = \{\rho\xi\}$	32
4.2.3 Is the Lebesgue Measure Invariant?	33
4.2.4 Frequency Analysis of $\mathcal{S}_2(\xi) = \{\rho\xi\}$	34
4.2.5 Estimate Invariant Density for $\mathcal{S}_2(\xi)$	35
4.2.6 Comparison with the Golden Ratio	35
4.3 Analysis of $\mathcal{S}_3(\xi) = \{\rho\xi\}$	37
4.3.1 Trajectory under $\mathcal{S}_3(\xi) = \{\rho\xi\}$	37

4.3.2	Perron Operator for $\mathcal{S}_3(\xi) = \{\rho\xi\}$	38
4.3.3	Is the Lebesgue Measure Invariant?	39
4.3.4	Frequency Analysis of $\mathcal{S}_3(\xi) = \{\rho\xi\}$	40
4.3.5	Estimate Invariant Density for $\mathcal{S}_3(\xi)$	41
4.3.6	Comparison with the Golden Ratio	41
5	Presentation of Software Code	45
5.1	Numerical Algorithm for Trajectory Generation	45
5.2	Algorithm for Plotting the Transformation $\mathcal{S}(\xi) = \{\rho\xi\}$	46
5.3	Algorithm for Frequency Histogram Computation	47
5.4	Algorithm for Invariant Density Estimation	48
5.5	Algorithm for Comparative Density Estimation of Irrational Maps	48
	Bibliography	50

List of Figures

4.1	Trajectory under $\mathcal{S}_1(\xi) = \{G\xi\}$ starting from $\xi_0 = 0.2$, where $G = \frac{1+\sqrt{5}}{2}$	23
4.2	Graph of the transformation $\mathcal{S}_1(\xi) = \{G\xi\}$ with $G = \frac{1+\sqrt{5}}{2}$. The vertical dashed line marks the discontinuity at $\xi = \frac{1}{G}$	24
4.3	Frequency distribution for $\mathcal{S}_1(\xi) = \{G\xi\}$ with $\xi_0 = \frac{\pi}{10}$, based on 20000 iterations and 50 equal bins.	29
4.4	Trajectory under $\mathcal{S}_2(\xi) = \{\rho\xi\}$ for $\rho = \frac{1}{2}(\sqrt{3} + 1)$ and $\xi_0 = 0.2$	31
4.5	Graph of the transformation $\mathcal{S}_2(\xi) = \{\rho\xi\}$ with $\rho = \frac{1+\sqrt{3}}{2}$. The dashed line marks the discontinuity at $\xi = \frac{1}{\rho}$	32
4.6	Frequency distribution for $\mathcal{S}_2(\xi) = \{\rho\xi\}$, $\rho = \frac{1}{2}(\sqrt{3} + 1)$, with $\xi_0 = \frac{\pi}{10}$ and 20000 iterations.	34
4.7	Estimated invariant density for the map $\mathcal{S}_2(\xi) = \{\rho\xi\}$, with $\rho = \frac{1+\sqrt{3}}{2}$	35
4.8	Estimated invariant densities for the maps $\mathcal{S}_2(\xi) = \{\rho\xi\}$ with $\rho = \frac{1+\sqrt{3}}{2}$ and $\mathcal{S}_1(\xi) = \{G\xi\}$ with the golden ratio $G = \frac{1+\sqrt{5}}{2}$	36
4.9	Trajectory under $\mathcal{S}_3(\xi) = \{\rho\xi\}$, with $\rho = \frac{1+\sqrt{7}}{2}$ and $\xi_0 = 0.2$	37
4.10	Graph of the transformation $\mathcal{S}_3(\xi) = \{\rho\xi\}$ with $\rho = \frac{1+\sqrt{7}}{2}$. The dashed line marks the discontinuity at $\xi = \frac{1}{\rho}$	38
4.11	Frequency distribution for $\mathcal{S}_3(\xi) = \{\rho\xi\}$, $\rho = \frac{1+\sqrt{7}}{2}$, with $\xi_0 = \frac{\pi}{10}$ and 20000 iterations.	40
4.12	Estimated invariant density for the map $\mathcal{S}_3(\xi) = \{\rho\xi\}$, with $\rho = \frac{1+\sqrt{7}}{2}$	41
4.13	Estimated invariant densities for the maps $\mathcal{S}_3(\xi) = \{\rho\xi\}$ with $\rho = \frac{1+\sqrt{7}}{2}$ and $\mathcal{S}_1(\xi) = \{G\xi\}$ with the golden ratio $G = \frac{1+\sqrt{5}}{2}$	42

List of Tables

1	List of Symbols Used in the Thesis	8
4.1	Trajectory of $\xi_n = \{1.618 \times \xi_{n-1}\}$ for $n = 0$ to 20	23
4.2	Trajectory of $\xi_n = \{1.366 \times \xi_{n-1}\}$ for $n = 0$ to 20	31
4.3	Trajectory of $\xi_n = \{1.8229 \times \xi_{n-1}\}$ for $n = 0$ to 20	37

List of Symbols

Table 1: List of Symbols Used in the Thesis

Symbol	Expression / Identity	Meaning
\mathcal{X}	$[0, 1)$	State space of the dynamical system
\mathcal{B}	—	Borel σ -algebra on $[0, 1)$
m	—	Lebesgue measure on \mathcal{B}
$\mathcal{S}(\xi)$	$\{\rho\xi\}$	Dynamical map with irrational $\rho > 1$
$\{\cdot\}$	$\{\xi\} = \xi - \lfloor \xi \rfloor$	Fractional part function
$\mathcal{S}_1(\xi)$	$\{G\xi\}$	Map with golden ratio
$\mathcal{S}_2(\xi)$	$\{\rho_2\xi\}$	Map with $\rho_2 = \frac{1+\sqrt{3}}{2}$
$\mathcal{S}_3(\xi)$	$\{\rho_3\xi\}$	Map with $\rho_3 = \frac{1+\sqrt{7}}{2}$
ρ	> 1 irrational	General parameter in $\mathcal{S}(\xi)$
G	$\frac{1+\sqrt{5}}{2}$	Golden ratio, approx. 1.618
ρ_2	$\frac{1+\sqrt{3}}{2}$	Approx. 1.366
ρ_3	$\frac{1+\sqrt{7}}{2}$	Approx. 1.823
$\psi(\xi)$	—	General density function on $[0, 1)$
$\psi_*(\xi)$	$P\psi_* = \psi_*$	Invariant density function
$P\psi$	—	Frobenius–Perron operator applied to ψ
$P1$	$P1(\xi)$	Operator applied to constant density
ξ_n	$\xi_n = \mathcal{S}(\xi_{n-1})$	n -th iterate of a trajectory
ξ_0	$\pi/10$	Initial point, approx. 0.314
n	—	Iteration index
m	$= 50$	Number of histogram bins
ψ_i	—	Relative frequency in i -th subinterval
μ_ψ	$\mu_\psi(A) = \int_A \psi dm$	Measure induced by ψ
$[a, b)$	$\subset [0, 1)$	Subinterval used in analysis

Introduction

The theory of dynamical systems provides a rigorous mathematical framework for describing how systems evolve over time. From Newton's deterministic laws of motion to modern theories of complexity and chaos, this field has undergone significant evolution [3, 6]. A dynamical system can be broadly defined as a tuple $(\mathcal{X}, \mathcal{B}, \mu, T)$, where \mathcal{X} is a measurable space, \mathcal{B} is a sigma-algebra on \mathcal{X} , μ is a measure (typically the Lebesgue measure), and $T : \mathcal{X} \rightarrow \mathcal{X}$ is a measurable transformation that determines the evolution of points in the space [4, 10].

This thesis focuses on a specific class of dynamical systems known as irrational rotations, given by

$$\mathcal{S}(\xi) = \{\rho\xi\}, \quad \xi \in [0, 1),$$

where $\{\cdot\}$ denotes the fractional part and ρ is an irrational constant such as the golden ratio $G = \frac{1+\sqrt{5}}{2}$, or other quadratic surds like $\frac{1+\sqrt{3}}{2}$ and $\frac{1+\sqrt{7}}{2}$. These transformations are linear and deterministic but exhibit rich behavior that is subtle and nontrivial [9, 1].

The main object of investigation in this thesis is the Perron operator associated with these maps. The Perron operator $P : L^1([0, 1), \mu) \rightarrow L^1([0, 1), \mu)$ is a fundamental tool in the study of measure-preserving and statistical properties of dynamical systems. For a measurable transformation $T : \mathcal{X} \rightarrow \mathcal{X}$, the operator is defined via

$$\int_A P\psi d\mu = \int_{T^{-1}(A)} \psi d\mu, \quad \text{for all } A \in \mathcal{B},$$

and describes the evolution of probability densities under the action of T [1, 9, 14]. This operator is linear, positive, and preserves the integral of densities, making it a special case of a Markov operator [12, 15]. While frequently applied in stochastic settings [5, 13, 18, 19], the Perron operator is equally essential for analyzing deterministic dynamics.

The primary aim of this thesis is to compute the Perron operator for maps of the form $\mathcal{S}(\xi) = \{\rho\xi\}$, where ρ is irrational, and to examine their invariant densities. In the case of the golden ratio, a known piecewise constant invariant density is recalled and verified. For the other values of ρ , namely $\frac{1+\sqrt{3}}{2}$ and $\frac{1+\sqrt{7}}{2}$, the invariant densities are estimated numerically via long orbit simulations and histogram-based frequency analysis.

The work builds on foundational insights from Lasota and Mackey [9], who emphasized that even simple deterministic systems can lead to complex statistical structures. Unlike the logistic map $\mathcal{S}(\xi) = 4\xi(1-\xi)$, which is nonlinear but Lebesgue measure preserv-

ing [4], the irrational rotation maps studied here are linear yet fail to preserve measure. Our results are supported by explicit operator derivations and graphical representations of numerically estimated densities (see Figures 4.2–4.10).

It is important to distinguish between equidistribution and measure preservation in this context. While irrational rotations $\mathcal{S}(\xi) = \{\rho\xi\}$ are known to produce equidistributed sequences in $[0, 1)$, as guaranteed by Weyl's criterion [10, 11], this property does not imply that the transformation preserves the Lebesgue measure. Our analysis makes this distinction precise by comparing theoretical equidistribution with practical deviations quantified through the Perron operator.

To summarize, the contributions of these thesis are:

- A derivation of the Perron operator for irrational rotations defined by specific quadratic surds;
- A presentation and verification of the known invariant density for the golden ratio map;
- Numerical estimation of invariant densities for transformations with $\rho = \frac{1+\sqrt{3}}{2}$ and $\rho = \frac{1+\sqrt{7}}{2}$;
- A clarification of the relationship between equidistribution, irrationality, and the non-invariance of the Lebesgue measure.

This investigation contributes to the broader understanding of how simple deterministic rules, when involving irrational constants, can lead to subtle and non-uniform statistical behaviors. These findings add to the growing literature on operator-theoretic approaches to dynamical systems [14, 15, 16, 13] and provide insights relevant to both pure and applied contexts, from number theory [17] to uncertainty quantification in complex systems [19].

Literature Review

The study of one-dimensional dynamical systems on the unit interval has evolved significantly, particularly through the development of operator-theoretic approaches for understanding the statistical behavior of iterated maps. A central tool in this context is the Perron operator, which describes how probability densities evolve under measurable transformations. Lasota and Yorke [1] and later Lasota and Mackey [9] laid the foundational theory for these operators in deterministic settings, showing how they encode global distributional dynamics that cannot be inferred from pointwise orbits alone. In particular, their work demonstrated how the operator framework enables the analysis of invariant densities and long-term statistical regularities across a wide range of transformations, including both chaotic and quasiperiodic systems.

Subsequent research has explored the behavior of the Perron operator under nonlinear transformations, such as the logistic map $\mathcal{S}(\xi) = 4\xi(1 - \xi)$, where the invariant density is explicitly given by $\psi(\xi) = \frac{1}{\pi\sqrt{\xi(1-\xi)}}$, and the Lebesgue measure is preserved [4]. This case stands in contrast to transformations of the form $\mathcal{S}(\xi) = \{\rho\xi\}$, where $\rho \in \mathbb{R} \setminus \mathbb{Q}$ is irrational. Such transformations, though linear and deterministic, often fail to preserve the Lebesgue measure, and the resulting invariant densities must be analyzed either analytically or numerically [13, 19].

The connection between number theory and dynamics is further emphasized in Weyl's theorem on equidistribution [11], which states that the sequence $\{n\rho\}$ for irrational ρ becomes uniformly distributed modulo 1. However, equidistribution of orbit sequences does not guarantee that the underlying transformation preserves measure. This subtle distinction motivates recent work that applies Perron operator theory to investigate the invariant structure of maps defined by irrational rotations.

Recent contributions have extended the application of these operators to stochastic systems and nonlinear optimization, underscoring their analytical versatility. For example, Hmissi [12] and Liu and Jiang [19] applied Perron–Frobenius techniques to random and uncertain dynamical systems, while Sahai [2] emphasized their utility in analyzing NP-hard problems. Other advancements include the approximation of Perron operator using spectral techniques and kernel methods, enabling more refined analysis in both deterministic and noisy contexts [13, 18].

This thesis draws upon the above developments by focusing on a class of irrational transformations defined as $\mathcal{S}_i(\xi) = \{\rho_i\xi\}$, where $\rho_i \in \left\{ \frac{1+\sqrt{5}}{2}, \frac{1+\sqrt{3}}{2}, \frac{1+\sqrt{7}}{2} \right\}$. For the case

$\rho = \frac{1+\sqrt{5}}{2}$, the invariant density is already known and is revisited here for verification and comparison. For the other two cases, where no closed-form expressions are available, invariant densities are estimated numerically. Numerical simulations of orbit trajectories and frequency histograms are used to approximate the statistical structure and support the theoretical conclusions, offering a detailed comparison between analytical reference and computational results.

2.1 Problem Statement

This study investigates a class of one-dimensional measurable dynamical systems defined on the unit interval $[0, 1)$, each generated by irrational rotations of the form

$$\mathcal{S}(\xi) = \{\rho\xi\}, \quad \rho > 1, \quad \rho \in \mathbb{R} \setminus \mathbb{Q},$$

where $\{\cdot\}$ denotes the fractional part function. Although governed by simple deterministic rules, these transformations exhibit intricate dynamical behavior, particularly in the context of their long-term statistical and measure-theoretic properties.

The primary focus is on the system $([0, 1), \mathcal{B}, m, \mathcal{S}_1)$, where $[0, 1)$ is the state space, \mathcal{B} is the Borel σ -algebra, m denotes the Lebesgue measure, and $\mathcal{S}_1(\xi) = \{G\xi\}$, with $G = \frac{1+\sqrt{5}}{2}$ representing the golden ratio. The central question addressed is whether this system preserves the Lebesgue measure and, if not, what type of invariant density it admits. In this case, a piecewise constant invariant density is derived analytically.

To extend the scope of analysis, two additional systems of the same form are examined: $\mathcal{S}_2(\xi) = \{\rho\xi\}$ with $\rho = \frac{1+\sqrt{3}}{2}$, and $\mathcal{S}_3(\xi) = \{\rho\xi\}$ with $\rho = \frac{1+\sqrt{7}}{2}$. All three transformations are piecewise linear and exhibit a discontinuity at $\xi = \frac{1}{\rho}$, a structural feature that induces nontrivial behavior in the evolution of densities.

Although linear and fully deterministic, these systems generate quasiperiodic, non-repeating trajectories under iteration. This research investigates both the qualitative and quantitative aspects of such dynamics, with particular emphasis on the existence and structure of invariant densities, the preservation (or failure) of Lebesgue measure, and the comparison between theoretical predictions and empirical distributions. For \mathcal{S}_2 and \mathcal{S}_3 , where no closed-form invariant densities were constructed, numerical estimation techniques based on long orbit simulations are employed to approximate the underlying invariant measures.

2.2 Research Objectives

The primary objective of this thesis is to explore the measure-theoretic and statistical properties of a class of one-dimensional dynamical systems defined by irrational rotations on the unit interval. These systems are modeled as $([0, 1), \mathcal{B}, m, \mathcal{S})$, where $\mathcal{S}(\xi) = \{\rho\xi\}$,

and ρ is an irrational number. The values of ρ considered in this study are $\frac{1+\sqrt{5}}{2}$ (the golden ratio), $\frac{1+\sqrt{3}}{2}$, and $\frac{1+\sqrt{7}}{2}$.

The first goal is to examine whether these transformations preserve the Lebesgue measure. To achieve this, the corresponding Perron operators are derived explicitly for each case, taking into account the piecewise definition of the transformation due to the discontinuity at $\xi = \frac{1}{\rho}$. By analyzing the operator's effect on the constant function $\psi(\xi) = 1$, the study establishes that none of the systems preserve the uniform measure.

The second objective is to determine the invariant densities associated with each transformation. For the golden ratio, the invariant density is already known and is included here for reference and comparison. In contrast, for the cases $\rho = \frac{1+\sqrt{3}}{2}$ and $\rho = \frac{1+\sqrt{7}}{2}$, the invariant densities for these systems are approximated numerically through orbit simulations and frequency histograms.

The final objective is to compare the analytical and numerical findings across the three systems, emphasizing how the arithmetic properties of ρ influence the form of the invariant measure. This comparative approach demonstrates that even simple fractional transformations with irrational multipliers can give rise to rich and varied statistical behavior. Ultimately, the study showcases the complementary power of analytical and numerical methods in the investigation of invariant measures in dynamical systems.

2.3 Thesis Outline

This thesis investigates the statistical and measure-theoretic properties of dynamical systems on the unit interval governed by irrational rotations of the form $\mathcal{S}(\xi) = \{\rho\xi\}$, where ρ is an irrational constant. Chapter 1 introduces the central research question and presents the motivation for analyzing such systems, beginning with historical developments in dynamics and progressing to modern density-based approaches using the Perron operator. It defines the problem of understanding how irrational linear transformations redistribute mass and potentially alter the Lebesgue measure. Chapter 2 provides a comprehensive literature review, covering foundational concepts from ergodic theory, operator theory, and number theory, and highlights key results on invariant measures, equidistribution, and the behavior of Perron operator in both linear and nonlinear systems. This chapter identifies the gap in existing research regarding the explicit construction of invariant densities for piecewise linear maps driven by irrational multipliers. Chapter 3 establishes the mathematical foundations necessary for the analysis, including formal definitions of measure spaces, measurable transformations, the Perron operator, and the properties of invariant measures. Chapter 4 presents the main analytical results of the thesis. It formally defines the dynamical systems $\mathcal{S}_1(\xi) = \{G\xi\}$, $\mathcal{S}_2(\xi) = \{\rho\xi\}$, and $\rho(\xi) = \{\eta\xi\}$, derives their associated Perron operator, examines whether they preserve the Lebesgue measure, and where estimate the invariant densities. These theoretical results are supported by numerical simulations of orbit trajectories and empirical histograms that validate the constructed

invariant measures. Chapter 5 concludes the thesis by summarizing the main contributions, discussing the influence of arithmetic properties of ρ on density evolution, and suggesting avenues for future research, including generalizations to higher-dimensional dynamics and stochastic perturbations.

Preliminary Notion

3.1 Measures and Measure Spaces

The formalization of measure theory provides the mathematical foundation for integrating functions, defining probability, and analyzing dynamical systems. Central to this theory is the notion of a *measure*—a set function that assigns a non-negative extended real number to subsets of a given space in a countably additive way. This section introduces the fundamental concepts of measures and measure spaces, which serve as the structural backbone for studying transformations, invariance, and ergodic behavior in measurable dynamics. We also review the properties of Borel sets, finite and probabilistic measure spaces, and the concepts of measurable and nonsingular transformations.

Definition 3.1.1 [See [9], Definition 2.1.2, page 18]

A real-valued function μ defined on a σ -algebra \mathcal{A} is a measure if:

(a) $\mu(\emptyset) = 0$;

(b) $\mu(A) \geq 0$ for all $A \in \mathcal{A}$; and

(c) $\mu(\bigcup_k A_k) = \sum_k \mu(A_k)$ if $\{A_k\}$ is a finite or infinite sequence of pairwise disjoint sets from \mathcal{A} , that is, $A_i \cap A_j = \emptyset$ for $i \neq j$.

Definition 3.1.2 [See [9], Definition 2.1.3, page 18]

The triple $(\mathcal{X}, \mathcal{A}, \mu)$ is referred to as a measure space if \mathcal{A} is a σ -algebra of subsets of \mathcal{X} and μ is a measure on \mathcal{A} . Since the measure is defined for the sets that belong to \mathcal{A} , they are referred to as measurable sets.

Remark 3.1.1 [See [9], Remark 2.1.3, page 18]

The sigma-algebra \mathcal{B} of Borel sets (the Borel sigma-algebra) is the most natural sigma-algebra if $\mathcal{X} = [0, 1]$ or \mathbb{R} . This is because it is the smallest sigma-algebra that contains intervals by definition. (The word "smallest" means that any other σ -algebra that contains intervals also contains any set in \mathcal{B} .) It can be showed that there is a unique measure μ on the Borel σ -algebra, known as the Borel measure, such that $\mu([a, b]) = b - a$.

Definition 3.1.3 [See [9], Definition 2.1.5, page 19]

If $\mu(\mathcal{X}) < \infty$, then a measure space $(\mathcal{X}, \mathcal{A}, \mu)$ is finite. More precisely, the measure space is normalized or probabilistic if $\mu(\mathcal{X}) = 1$.

Definition 3.1.4 [See [9], Definition No. 3.2.1, page 41]

Consider $(\mathcal{X}, \mathcal{A}, \mu)$ be a measure space. A transformation $\mathcal{S} : \mathcal{X} \rightarrow \mathcal{X}$ is said to be measurable if

$$\mathcal{S}^{-1}(A) \in \mathcal{A} \quad \forall \quad A \in \mathcal{A}.$$

Definition 3.1.5 [See [9], Definition 3.2.2, page 41] Consider a measure space $(\mathcal{X}, \mathcal{A}, \mu)$, A measurable transformation $\mathcal{S} : \mathcal{X} \rightarrow \mathcal{X}$ is nonsingular if

$$\mu(\mathcal{S}^{-1}(A)) = 0 \quad \forall \quad A \in \mathcal{A} \text{ such that } \mu(A) = 0.$$

3.1.1 Perron Operator

The Perron operator is essential for characterising the development of densities under a specific transformation in the study of dynamical systems. Given a nonsingular transformation on a measure space, the Perron operator provides a mechanism for transferring information about the distribution of mass across measurable sets. This section introduces the definition and key properties of the Perron operator, both in abstract formulation and in specific computable cases. Emphasis is placed on its linearity, positivity-preserving nature, and its role in preserving integrals. We also present an explicit example involving a transformation on the unit interval to illustrate the operator's behavior and implications in ergodic and probabilistic contexts.

Definition 3.1.6 (See [4], Definition 3.2.3, page 15) A dynamical system is a quadruple $(\mathcal{X}, \mathcal{A}, \mu, \mathcal{S})$, where $(\mathcal{X}, \mathcal{A}, \mu)$ is a measurable space and $\mathcal{S} : \mathcal{X} \rightarrow \mathcal{X}$ is a nonsingular transformation of this space.

Definition 3.1.7 (See [4], Definition 3.2.3, page 15) Let $(\mathcal{X}, \mathcal{A}, \mu, \mathcal{S})$ be a dynamical system. An operator $P : L^1(\mathcal{X}, \mathcal{A}, \mu) \rightarrow L^1(\mathcal{X}, \mathcal{A}, \mu)$ is called the Perron operator corresponding to the transformation \mathcal{S} if the subsequent criteria are fulfilled.:

(a) for any $\psi \in L^1$, $\psi \geq 0$ the equality

$$\int_A P\psi(\xi) \mu(dx) = \int_{\mathcal{S}^{-1}(A)} \psi(\xi) \mu(dx)$$

holds for all $A \in \mathcal{A}$;

(b) for any $\psi \in L^1$

$$P\psi = P\psi^+ - P\psi^-.$$

Definition 3.1.8 [See [4], Definition B 3.2.4, page 16]

Let A dynamical system $(\mathcal{X}, \mathcal{A}, \mu, \mathcal{S})$ be considered. An operator $P : L^1(\mathcal{X}, \mathcal{A}, \mu) \rightarrow L^1(\mathcal{X}, \mathcal{A}, \mu)$ is called the Perron operator corresponding to the transformation \mathcal{S} if for all functions $\psi \in L^1(\mathcal{X}, \mathcal{A}, \mu)$ and all $A \in \mathcal{A}$

$$\int_A P\psi(\xi) \mu(dx) = \int_{\mathcal{S}^{-1}(A)} \psi(\xi) \mu(dx).$$

It is elementary to demonstrate that P possesses the following characteristics:

(FP1) $P(\lambda_1\psi_1 + \lambda_2\psi_2) = \lambda_1P\psi_1 + \lambda_2P\psi_2$ for all $\psi_1, \psi_2 \in L^1$, $\lambda_1, \lambda_2 \in \mathbb{R}$, so P is a linear operator;

(FP2) $P\psi \geq 0$ if and only if $\psi \geq 0$; and

(FP3) $\int_{\mathcal{X}} P\psi(\xi) \mu(dx) = \int_{\mathcal{X}} \psi(\xi) \mu(dx)$;

(FP4) If $\mathcal{S}_n = \mathcal{S}_0 \circ \cdots \circ \mathcal{S}$ and P_n is the Perron operator corresponding to \mathcal{S}_n , then $P_n = P_0 \cdots P$, where P is the Perron operator corresponding to \mathcal{S} .

In some special cases, If $\mathcal{X} = (a, b]$ is an interval on the real line \mathbb{R} , and $\mathcal{A} = \{[a, \xi] : \xi \in (a, b]\}$, then

$$\int_a^\xi P\psi(s) ds = \int_{\mathcal{S}^{-1}((a, \xi])} \psi(s) ds, \quad (3.1)$$

and by differentiating,

$$P\psi(\xi) = \frac{d}{dx} \int_{\mathcal{S}^{-1}((a, \xi])} \psi(s) ds. \quad (3.2)$$

It should be noted that an explicit form for $P\psi$ exists in cases where the transformation \mathcal{S} is differentiable and invertible. It follows that \mathcal{S} must be monotone if it is both differentiable and invertible. Assume that \mathcal{S} is an increasing function and that the derivative of \mathcal{S}^{-1} is continuous. Then

$$\mathcal{S}^{-1}([a, \xi]) = (\mathcal{S}^{-1}(a), \mathcal{S}^{-1}(\xi)], \quad (3.3)$$

from (3.2)

$$P\psi(\xi) = \frac{d}{dx} \int_{\mathcal{S}^{-1}(a)}^{\mathcal{S}^{-1}(\xi)} \psi(s) ds = \psi(\mathcal{S}^{-1}(\xi)) \cdot \frac{d}{dx} \mathcal{S}^{-1}(\xi). \quad (3.4)$$

Example 3.1.1 [See [4], Example 3.2.1, page 19]

The transformation $\mathcal{S}: [0, 1] \rightarrow [0, 1]$ is defined by $\mathcal{S}(\xi) = 2\xi \bmod 1 = \{2\xi\}$. Take the measure space $(\mathcal{X}, \mathcal{A}, \mu) = ([0, 1], \mathcal{B}, m)$. The objective is to determine the Perron operator's explicit form in relation to this transformation.

We find that the preimage of the interval $[0, \xi]$ under \mathcal{S} is $\mathcal{S}^{-1}([0, \xi]) = \{2t\}$ is given by

$$\mathcal{S}^{-1}([0, \xi]) = \left[0, \frac{\xi}{2}\right] \cup \left[\frac{1}{2}, \frac{1}{2} + \frac{\xi}{2}\right].$$

Applying the general formula for the Perron operator, we obtain

$$P\psi(\xi) = \left(\int_0^{\frac{\xi}{2}} \psi(y) dy + \int_{\frac{1}{2}}^{\frac{\xi}{2} + \frac{1}{2}} \psi(y) dy \right)'_{\xi} = \frac{1}{2} \left(\psi\left(\frac{\xi}{2}\right) + \psi\left(\frac{\xi}{2} + \frac{1}{2}\right) \right),$$

for any integrable function $\psi \in L^1([0, 1], \mathcal{B}, m)$.

Let us now take $\psi_0(\xi) = \xi$. Applying the operator P , we obtain

$$P\psi_0(\xi) = \frac{\xi}{2} + \frac{1}{4} = \psi_1(\xi).$$

Proceeding to the second iterate

$$P^2\psi_0(\xi) = P(\psi_1(\xi)) = \frac{1}{2} \left(\frac{\xi}{4} + \frac{1}{4} \right) + \frac{1}{2} \left(\frac{\frac{\xi}{2} + \frac{1}{2}}{2} + \frac{1}{4} \right) = \frac{\xi}{4} + \frac{3}{8}.$$

Continuing this process inductively, we find that

$$P^n\psi_0(\xi) = \frac{\xi}{2^n} + \frac{2^n - 1}{2^{n+1}},$$

for any natural number n .

Now, consider the function

$$\psi_1(\xi) = \begin{cases} 1, & \text{if } 0 \leq \xi \leq \frac{1}{2}, \\ -1, & \text{if } \frac{1}{2} \leq \xi \leq 1. \end{cases}$$

For this function, we observe that

$$P\psi_1(\xi) = 0 \quad \text{for all } \xi \in [0, 1].$$

This example illustrates that, in general, it is possible for the Perron operator to yield zero on a set A , even when the original function ψ is non-zero on the full preimage $\mathcal{S}^{-1}(A)$. Specifically, in this case

$$P\psi(\xi) = 0 \quad \text{for all } \xi \in A \quad \text{yet} \quad \psi(\xi) \neq 0 \quad \text{for all } \xi \in \mathcal{S}^{-1}(A),$$

as demonstrated by the fact that $P\psi_1(\xi) = 0$ for all $\xi \in [0, 1]$, despite $\psi_1(\xi) \neq 0$ on all of $[0, 1] = \mathcal{S}^{-1}([0, 1])$.

3.2 Invariant Measures and Measure-Preserving Transformations

Invariant measures provide a framework for analyzing how transformations affect the distribution of mass within a measurable space. A transformation is said to be measure-preserving if it leaves the measure unchanged under preimages of measurable sets, ensuring that the total measure remains constant through the dynamics. This section introduces the formal definition of measure-preserving transformations and discusses the conditions under which a measure remains invariant. Specifically, we look at how the Perron operator

helps find invariant densities and provide examples, such as the r -adic and quadratic transformations, to illustrate these concepts in both simple and nontrivial cases. The exposition follows the foundational treatments in [4, 9].

Definition 3.2.1 [See [4], Definition 4.1.1, page 25] Let $(\mathcal{X}, \mathcal{A}, \mu, \mathcal{S})$ be a dynamical system. It is said that the transformation \mathcal{S} is measure-preserving if

$$\mu(\mathcal{S}^{-1}(A)) = \mu(A)$$

$$\forall A \in \mathcal{A}$$

This condition implies that the measure μ remains unchanged under the action of \mathcal{S} . In other words, \mathcal{S} is said to be measure-preserving with respect to the measure μ , and conversely, μ is said to be invariant under \mathcal{S} . Furthermore, any measure-preserving transformation is necessarily *nonsingular*, since for any measurable set A with $\mu(A) = 0$, the invariance condition ensures that $\mu(\mathcal{S}^{-1}(A)) = 0$ as well.

The following theorem establishes a criterion for determining whether a transformation preserves a given measure, using the Perron–Frobenius operator.

Theorem 3.2.1 [See [4], Theorem 4.1.1, page 25] Let $(\mathcal{X}, \mathcal{A}, \mu, \mathcal{S})$ be a dynamical system, and let P denote the Perron–Frobenius operator associated with the transformation \mathcal{S} . Suppose that $\psi \in L^1(\mathcal{X}, \mathcal{A}, \mu)$ with $\psi > 0$. Define a new measure μ_ψ on $(\mathcal{X}, \mathcal{A})$ by

$$\mu_\psi(A) = \int_A \psi(\xi) \mu(dx).$$

Then, the measure μ_ψ is invariant under \mathcal{S} if and only if, ψ is a fixed point of the operator P , i.e., $P\psi = \psi$.

Theorem 3.2.2 [See [4], Theorem 4.1.1, page 52] Let $(\mathcal{X}, \mathcal{A}, \mu)$ be a measure space, $\mathcal{S} : \mathcal{X} \rightarrow \mathcal{X}$ a nonsingular transformation, and P the Frobenius–Perron operator associated with \mathcal{S} . Consider a nonnegative $\psi \in L^1$. Then a measure μ_ψ given by

$$\mu_\psi(A) = \int_A \psi(\xi) \mu(dx) \tag{3.5}$$

is invariant if and only if ψ is a fixed point of P .

Remark 3.2.1 [See [4], Remark 4.1.1, page 52] Note that the original measure μ is invariant if and only if $P1 = 1$.

Example 3.2.1 [See [1], Example 1.2.1, page 8]

Consider the transformation $\mathcal{S} : [0, 1] \rightarrow [0, 1]$ given by

$$\mathcal{S}(\xi) = r\xi \pmod{1}, \tag{3.6}$$

where r is an integer. The notation $rx \pmod{1}$ means $rx - n$, where n is the largest integer such that $rx - n \geq 0$. This expression is customarily called the r -adic transformation.

Example 3.2.2 [See [9], Example 4.1.1, page 52] Consider the r -adic transformation originally introduced in Example 3.2.1,

$$\mathcal{S}(\xi) = r\xi \pmod{1},$$

where $r > 1$ is an integer, on the measure space $([0, 1], \mathcal{B}, \mu)$ where \mathcal{B} is the Borel σ -algebra and μ is the Borel measure. For any interval $[0, \xi] \subseteq [0, 1]$,

$$\mathcal{S}^{-1}([0, \xi]) = \bigcup_{i=0}^{r-1} \left[\frac{i}{r}, \frac{\xi + i}{r} \right],$$

and the Frobenius-Perron operator P corresponding to \mathcal{S} is given by

$$P\psi(\xi) = \frac{1}{r} \sum_{i=0}^{r-1} \psi \left(\frac{\xi + i}{r} \right). \quad (3.7)$$

Thus,

$$P1 = \frac{1}{r} \sum_{i=0}^{r-1} 1 = 1,$$

and by our previous remark the Borel measure is invariant under the r -adic transformation.

Remark 3.2.2 [See [9], Remark 4.1.2, page 53] It should be noted that, as defined, the r -adic transformation is not continuous at 1. However, if instead of defining the r -adic transformation on the interval $[0, 1]$ we define it on the unit circle (circle with circumference 1) obtained by identifying 0 with 1 on the interval $[0, 1]$, then it is continuous and differentiable throughout.

Example 3.2.3 [See [9], Example 4.1.2, page 53] Again consider the measure space $([0, 1], \mathcal{B}, \mu)$ where μ is the Borel measure. Let $\mathcal{S} : [0, 1] \rightarrow [0, 1]$ be the quadratic map $\mathcal{S}(\xi) = 4\xi(1 - \xi)$. For $[0, \xi] \subseteq [0, 1]$,

$$\mathcal{S}^{-1}([0, \xi]) = \left[0, \frac{1 - \sqrt{1 - \xi}}{2} \right] \cup \left[\frac{1 + \sqrt{1 - \xi}}{2}, 1 \right],$$

and the Frobenius-Perron operator is given by

$$P\psi(\xi) = \frac{1}{4\sqrt{1 - \xi}} \left(\psi \left(\frac{1 - \sqrt{1 - \xi}}{2} \right) + \psi \left(\frac{1 + \sqrt{1 - \xi}}{2} \right) \right).$$

Clearly,

$$P1 = \frac{1}{2\sqrt{1 - \xi}} \neq 1,$$

So the Borel measure μ is not invariant under \mathcal{S} by Remark 3.2.1. To find an invariant measure, we must find a solution to $P\psi = \psi$, that is,

$$\psi_*(\xi) = \frac{1}{\pi\sqrt{\xi(1-\xi)}}, \quad (3.8)$$

which was first solved by Ulam and von Neumann (1947). It is straightforward to verify that ψ_* given by (3.8) indeed satisfies $P\psi = \psi$. Hence, the measure

$$\mu_{\psi_*}(A) = \int_A \frac{1}{\pi\sqrt{\xi(1-\xi)}} dx$$

is invariant under the quadratic transformation $\mathcal{S}(\xi) = 4\xi(1-\xi)$.

Remark 3.2.3 [See [9], Remark 4.1.3, page 53] The factor of π in equation (3.8) ensures that ψ_* is a valid probability density function, and thus that the measure μ_{ψ_*} is normalized.

Study of a single dynamical system

This chapter examines a family of dynamical systems defined on the unit interval $[0, 1)$, generated by transformations of the form

$$\mathcal{S}(\xi) = \{\rho\xi\}, \quad \rho > 1,$$

where $\{\cdot\}$ denotes the fractional part and ρ is an irrational number. These systems are analyzed using the Perron operator, which describes how probability densities evolve under the transformation and provides the key to identifying invariant measures. The map \mathcal{S} is piecewise linear with a single discontinuity at $\xi = \frac{1}{\rho}$, dividing the interval into two regions governed by distinct linear expressions.

Three specific irrational parameters are investigated: the golden ratio $\rho = \frac{1+\sqrt{5}}{2}$, $\rho = \frac{1+\sqrt{3}}{2}$, and $\rho = \frac{1+\sqrt{7}}{2}$. For each case, the Perron operator is derived explicitly, and it is demonstrated that the Lebesgue measure is not invariant under the corresponding transformation.

In the case of the golden ratio, a known piecewise constant invariant density is presented and verified. For the other two values, numerical methods were used to estimate their statistical behavior. Specifically, frequency histograms of orbit iterates are constructed over long time spans to approximate the invariant measure. These histograms revealed smoothly varying density profiles, in contrast to the piecewise constant structure seen in the golden ratio case.

Graphical illustrations of each transformation and its associated density are included to highlight the dynamical behavior and structural distinctions among the three systems. The comparison underscores how different irrational multipliers lead to markedly different invariant measures, despite the shared form of the underlying transformation.

4.1 Analysis of $\mathcal{S}_1(\xi) = \{G\xi\}$

4.1.1 Trajectory under $\mathcal{S}_1(\xi) = \{G\xi\}$

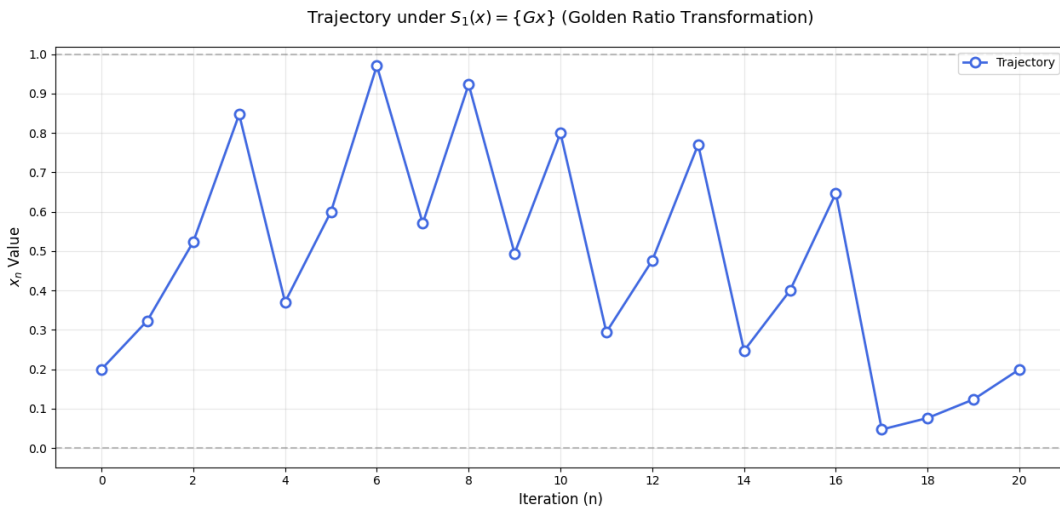
Analyze the population trajectory for the map $\mathcal{S}_1(\xi) = \{G\xi\}$, where $G = \frac{1+\sqrt{5}}{2}$ (the golden ratio), and the initial state $\xi_0 = 0.2$. The fractional part $\{G\xi\}$ is equivalent to $G\xi \pmod{1}$.

The trajectory for ξ_n from $n = 0$ to $n = 20$ is computed as follows

Figure 4.1 illustrates the trajectory of the point $\xi_0 = 0.2$ under the transformation

Table 4.1: Trajectory of $\xi_n = \{1.618 \times \xi_{n-1}\}$ for $n = 0$ to 20

n	Computation	ξ_n value
0	—	0.2000
1	$\{1.618 \times 0.2000\} = \{0.3236\}$	0.3236
2	$\{1.618 \times 0.3236\} \approx \{0.5236\}$	0.5236
3	$\{1.618 \times 0.5236\} \approx \{0.8472\}$	0.8472
4	$\{1.618 \times 0.8472\} \approx \{1.3712\}$	0.3712
5	$\{1.618 \times 0.3712\} \approx \{0.6007\}$	0.6007
6	$\{1.618 \times 0.6007\} \approx \{0.9719\}$	0.9719
7	$\{1.618 \times 0.9719\} \approx \{1.5726\}$	0.5726
8	$\{1.618 \times 0.5726\} \approx \{0.9265\}$	0.9265
9	$\{1.618 \times 0.9265\} \approx \{1.4991\}$	0.4991
10	$\{1.618 \times 0.4991\} \approx \{0.8076\}$	0.8076
11	$\{1.618 \times 0.8076\} \approx \{1.3067\}$	0.3067
12	$\{1.618 \times 0.3067\} \approx \{0.4963\}$	0.4963
13	$\{1.618 \times 0.4963\} \approx \{0.8030\}$	0.8030
14	$\{1.618 \times 0.8030\} \approx \{1.2993\}$	0.2993
15	$\{1.618 \times 0.2993\} \approx \{0.4843\}$	0.4843
16	$\{1.618 \times 0.4843\} \approx \{0.7836\}$	0.7836
17	$\{1.618 \times 0.7836\} \approx \{1.2679\}$	0.2679
18	$\{1.618 \times 0.2679\} \approx \{0.4335\}$	0.4335
19	$\{1.618 \times 0.4335\} \approx \{0.7014\}$	0.7014
20	$\{1.618 \times 0.7014\} \approx \{1.1349\}$	0.1349


 Figure 4.1: Trajectory under $\mathcal{S}_1(\xi) = \{G\xi\}$ starting from $\xi_0 = 0.2$, where $G = \frac{1+\sqrt{5}}{2}$.

$\mathcal{S}_1(\xi) = \{G\xi\}$, where $G = \frac{1+\sqrt{5}}{2}$. The plot shows the evolution of the orbit ξ_n over 20 iterations. As expected for irrational rotations, the sequence does not settle into a fixed point or periodic cycle, but rather exhibits quasiperiodic behavior, spreading over the interval $[0, 1)$. This visual confirms that the orbit remains bounded within the unit interval and reflects the non-repeating nature of the map induced by the irrational multiplier.

4.1.2 Perron Operator for $\mathcal{S}_1(\xi) = \{G\xi\}$

Consider the dynamical system $([0, 1), \mathcal{B}, m, \mathcal{S}_1)$, where

$$\mathcal{S}_1(\xi) = \{G\xi\}, \quad G = \frac{1 + \sqrt{5}}{2}.$$

The map $\mathcal{S}_1(\xi) = \{G\xi\}$ is the fractional part of $G\xi$, defined by:

$$\mathcal{S}_1(\xi) = \begin{cases} G\xi, & \text{if } 0 \leq \xi < \frac{1}{G}, \\ G\xi - 1, & \text{if } \frac{1}{G} \leq \xi < 1. \end{cases}$$

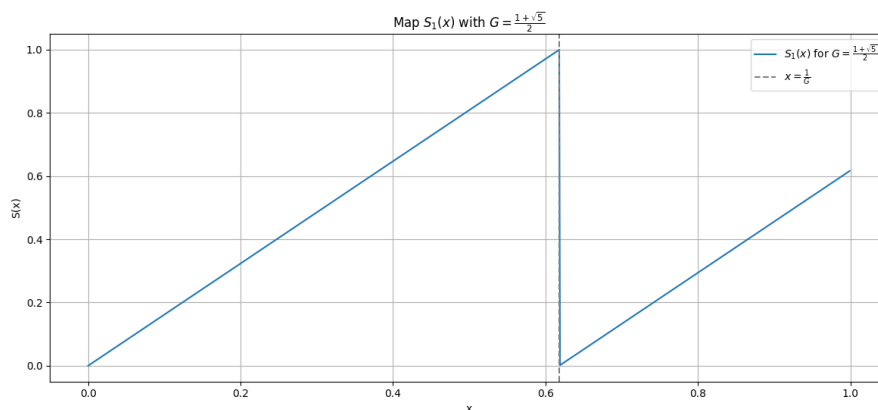


Figure 4.2: Graph of the transformation $\mathcal{S}_1(\xi) = \{G\xi\}$ with $G = \frac{1+\sqrt{5}}{2}$. The vertical dashed line marks the discontinuity at $\xi = \frac{1}{G}$.

Compute the Perron operator $P\psi$ associated with \mathcal{S}_1 , using the definition

$$P\psi(\xi) = \frac{d}{dx} \int_{\mathcal{S}_1^{-1}([0, \xi])} \psi(u) du.$$

Analyze the set of preimages of $[0, \xi]$ under the transformation \mathcal{S}_1 ,

$$\mathcal{S}_1^{-1}([0, \xi]) = \{u \in [0, 1) : \mathcal{S}_1(u) \in [0, \xi]\}.$$

now consider the map piecewise

Branch 1: $\mathcal{S}_1(u) = Gu$

This is valid when $u \in [0, \frac{1}{G})$. To satisfy $\mathcal{S}_1(u) = Gu \in [0, \xi]$, it is required that

$$0 \leq Gu \leq \xi \quad \Rightarrow \quad u \in \left[0, \frac{\xi}{G}\right].$$

However, u must also satisfy $u < \frac{1}{G}$, so

$$u \in \left[0, \min\left(\frac{\xi}{G}, \frac{1}{G}\right)\right].$$

Branch 2: $\mathcal{S}_1(u) = Gu - 1$

This is valid when $u \in [\frac{1}{G}, 1)$. We require

$$0 \leq Gu - 1 \leq \xi \quad \Rightarrow \quad 1 \leq Gu \leq 1 + \xi \quad \Rightarrow \quad u \in \left[\frac{1}{G}, \frac{1 + \xi}{G}\right].$$

Again, since $u < 1$, the valid preimage from this branch is

$$u \in \left[\frac{1}{G}, \min\left(\frac{1 + \xi}{G}, 1\right)\right].$$

Combining both branches, the total preimage is

$$\mathcal{S}_1^{-1}([0, \xi]) = \left[0, \min\left(\frac{\xi}{G}, \frac{1}{G}\right)\right] \cup \left[\frac{1}{G}, \min\left(\frac{1 + \xi}{G}, 1\right)\right].$$

compute

$$P\psi(\xi) = \frac{d}{dx} \int_{\mathcal{S}_1^{-1}([0, \xi])} \psi(u) du.$$

by analyzing two cases.

Case 1: $\xi \in [0, \frac{1}{G})$

Here

$$\frac{\xi}{G} < \frac{1}{G}, \quad \frac{1 + \xi}{G} < 1,$$

so

$$\mathcal{S}_1^{-1}([0, \xi]) = \left[0, \frac{\xi}{G}\right] \cup \left[\frac{1}{G}, \frac{1 + \xi}{G}\right].$$

Then

$$\int_{\mathcal{S}_1^{-1}([0, \xi])} \psi(u) du = \int_0^{\xi/G} \psi(u) du + \int_{1/G}^{(1+\xi)/G} \psi(u) du.$$

Using Leibniz's rule

$$\begin{aligned} \frac{d}{dx} \int_0^{\xi/G} \psi(u) du &= \frac{1}{G} \psi\left(\frac{\xi}{G}\right), \\ \frac{d}{dx} \int_{1/G}^{(1+\xi)/G} \psi(u) du &= \frac{1}{G} \psi\left(\frac{1 + \xi}{G}\right). \end{aligned}$$

Therefore

$$P\psi(\xi) = \frac{1}{G} \psi\left(\frac{\xi}{G}\right) + \frac{1}{G} \psi\left(\frac{1 + \xi}{G}\right), \quad \text{for } \xi \in \left[0, \frac{1}{G}\right).$$

Case 2: $\xi \in [\frac{1}{G}, 1)$

In this case

$$\frac{\xi}{G} < \frac{1}{G}, \quad \frac{1+\xi}{G} > 1.$$

Hence, second branch preimage $[\frac{1}{G}, \frac{1+\xi}{G}]$ overshoots 1 and is truncated at 1, so:

$$\min\left(\frac{1+\xi}{G}, 1\right) = 1 \quad \Rightarrow \text{upper limit exceeds domain.}$$

But since $\frac{1+\xi}{G} \geq 1$, the second integral vanishes (or contributes zero to derivative), and we only retain

$$\mathcal{S}_1^{-1}([0, \xi]) = \left[0, \frac{\xi}{G}\right].$$

Therefore

$$P\psi(\xi) = \frac{d}{dx} \int_0^{\xi/G} \psi(u) du = \frac{1}{G} \psi\left(\frac{\xi}{G}\right), \quad \text{for } \xi \in \left[\frac{1}{G}, 1\right).$$

Combining both cases, we obtain

$$P\psi(\xi) = \begin{cases} \frac{1}{G} \left[\psi\left(\frac{\xi}{G}\right) + \psi\left(\frac{1+\xi}{G}\right) \right], & \text{if } \xi \in [0, \frac{1}{G}), \\ \frac{1}{G} \psi\left(\frac{\xi}{G}\right), & \text{if } \xi \in [\frac{1}{G}, 1). \end{cases}$$

This is the Perron operator for the transformation $\mathcal{S}_1(\xi) = \{G\xi\}$ on $[0, 1)$.

Let $G = \frac{1+\sqrt{5}}{2}$ be the golden ratio. Define the transformation

$$\mathcal{S}_1(\xi) = \{G\xi\} = \begin{cases} G\xi, & \text{if } \xi \in [0, \frac{1}{G}), \\ G\xi - 1, & \text{if } \xi \in [\frac{1}{G}, 1). \end{cases}$$

The associated Perron operator is:

$$P\psi(\xi) = \begin{cases} \frac{1}{G} \left[\psi\left(\frac{\xi}{G}\right) + \psi\left(\frac{1+\xi}{G}\right) \right], & \xi \in [0, \frac{1}{G}) \\ \frac{1}{G} \psi\left(\frac{\xi}{G}\right), & \xi \in [\frac{1}{G}, 1) \end{cases}$$

4.1.3 Is the Lebesgue Measure Invariant?

To check whether the Lebesgue measure is invariant by checking whether the constant function $\psi(\xi) = 1$ satisfies $P\psi(\xi) = 1$.

Case 1: $\xi \in [0, \frac{1}{G})$

$$P\psi(\xi) = \frac{1}{G} [1 + 1] = \frac{2}{G} \approx 1.236$$

Case 2: $\xi \in [\frac{1}{G}, 1)$

$$P\psi(\xi) = \frac{1}{G} \cdot 1 = \frac{1}{G} \approx 0.618$$

Since

$$P\psi(\xi) = \begin{cases} > 1, & \xi \in [0, \frac{1}{G}) \\ < 1, & \xi \in [\frac{1}{G}, 1) \end{cases}$$

the constant function is not invariant. Hence, the Lebesgue measure is not preserved by $\mathcal{S}_1(\xi)$.

4.1.4 Invariant Density of $\mathcal{S}_1(\xi)$

We now seek a piecewise constant density function:

$$\psi(\xi) = \begin{cases} a, & \xi \in [0, \frac{1}{G}) \\ b, & \xi \in [\frac{1}{G}, 1) \end{cases}$$

such that $P\psi(\xi) = \psi(\xi)$.

Case 1: $\xi \in [0, \frac{1}{G})$

Using the operator

$$P\psi(\xi) = \frac{1}{G} \left[\psi\left(\frac{\xi}{G}\right) + \psi\left(\frac{1+\xi}{G}\right) \right]$$

Now analyze where these values lie

- $\frac{\xi}{G} \in [0, \frac{1}{G^2}) \subset [0, \frac{1}{G}) \Rightarrow \psi\left(\frac{\xi}{G}\right) = a$
- $\frac{1+\xi}{G} \in [\frac{1}{G}, 1) \Rightarrow \psi\left(\frac{1+\xi}{G}\right) = b$

So

$$P\psi(\xi) = \frac{1}{G}(a + b)$$

But since $\psi(\xi) = a$ in this region, we require

$$a = \frac{a + b}{G} \tag{4.1}$$

Case 2: $\xi \in [\frac{1}{G}, 1)$

Using the operator

$$P\psi(\xi) = \frac{1}{G} \psi\left(\frac{\xi}{G}\right)$$

Now, $\frac{\xi}{G} \in [\frac{1}{G^2}, \frac{1}{G}) \subset [0, \frac{1}{G}) \Rightarrow \psi(\frac{\xi}{G}) = a$

So

$$P\psi(\xi) = \frac{1}{G}a$$

But since $\psi(\xi) = b$ here, we require

$$b = \frac{a}{G} \tag{4.2}$$

Solving the System

From (4.2): $a = bG$

Substitute into (4.1):

$$bG = \frac{bG + b}{G} = b \cdot \frac{G + 1}{G} \Rightarrow G = \frac{G + 1}{G} \Rightarrow G^2 = G + 1$$

This identity holds since $G = \frac{1+\sqrt{5}}{2}$. So the structure is consistent.

by imposing the condition

$$\int_0^1 \psi(\xi) dx = 1 \Rightarrow a \cdot \frac{1}{G} + b \cdot \left(1 - \frac{1}{G}\right) = 1$$

Using $a = bG$ and $1 - \frac{1}{G} = \frac{1}{G^2}$

$$bG \cdot \frac{1}{G} + b \cdot \frac{1}{G^2} = b \left(1 + \frac{1}{G^2}\right)$$

Now

$$1 + \frac{1}{G^2} = \frac{G^2 + 1}{G^2} \Rightarrow b = \frac{G^2}{G^2 + 1}$$

Then

$$a = bG = \frac{G^3}{G^2 + 1}$$

Recall $G^2 = G + 1$,

$$G^2 + 1 = G + 2, \quad G^3 = G(G^2) = G(G + 1) = G^2 + G = 2G + 1$$

hence

$$a = \frac{2G + 1}{G + 2}, \quad b = \frac{G + 1}{G + 2}$$

Thus, the invariant density is

$$\psi(\xi) = \begin{cases} \frac{2G + 1}{G + 2}, & \xi \in [0, \frac{1}{G}) \\ \frac{G + 1}{G + 2}, & \xi \in [\frac{1}{G}, 1) \end{cases}$$

This density satisfies:

$$P\psi(\xi) = \psi(\xi), \quad \int_0^1 \psi(\xi) dx = 1$$

and is therefore the unique invariant density for $\mathcal{S}_1(\xi) = \{G\xi\}$.

4.1.5 Frequency Analysis of $\mathcal{S}_1(\xi) = \{G\xi\}$

For the irrational rotation $\mathcal{S}_1(\xi) = \{G\xi\}$ where $G = \frac{1+\sqrt{5}}{2}$,

Divide $[0, 1)$ into $m = 50$ equal subintervals

$$[0, 1) = \bigcup_{i=1}^{20} \left[\frac{i-1}{20}, \frac{i}{20} \right)$$

Take initial condition $\xi_0 = \frac{\pi}{10} \approx 0.314$

Compute trajectory for $n = 20000$ iterations

$$\xi_0, \mathcal{S}_1(\xi_0), \mathcal{S}_1^2(\xi_0), \dots, \mathcal{S}_1^{20000}(\xi_0)$$

Calculate visit frequencies

$$\psi_i = \frac{1}{20000} \times \# \left\{ 1 \leq j \leq 20000 \mid \mathcal{S}_1^j(\xi_0) \in \left[\frac{i-1}{20}, \frac{i}{20} \right) \right\}$$

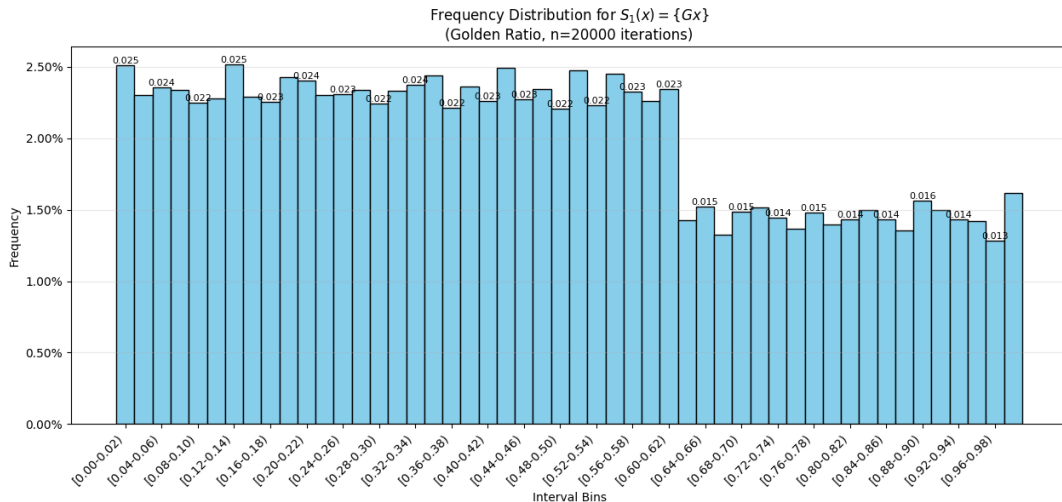


Figure 4.3: Frequency distribution for $\mathcal{S}_1(\xi) = \{G\xi\}$ with $\xi_0 = \frac{\pi}{10}$, based on 20000 iterations and 50 equal bins.

Figure 4.3 presents the frequency distribution of the orbit of $\xi_0 = \frac{\pi}{10} \approx 0.314$ under the transformation $\mathcal{S}_1(\xi) = \{G\xi\}$, where $G = \frac{1+\sqrt{5}}{2}$. The unit interval $[0, 1)$ is partitioned into 50 equal subintervals, and the number of visits to each bin over 20000 iterations is recorded. The resulting histogram reflects how the orbit is distributed across the interval.

While the distribution is not perfectly uniform, the frequencies are generally consistent with the structure of the invariant measure, highlighting a mild asymmetry introduced by the discontinuity at $\xi = \frac{1}{G}$. This empirical result supports the analytic form of the invariant density derived earlier.

4.2 Analysis of $\mathcal{S}_2(\xi) = \{\rho\xi\}$

4.2.1 Trajectory under $\mathcal{S}_2(\xi) = \{\rho\xi\}$

Analyze the population trajectory for the map $\mathcal{S}_2(\xi) = \{\rho\xi\}$, where $\rho = \frac{1}{2}(\sqrt{3} + 1)$, and the initial state $\xi_0 = 0.2$. The fractional part $\{\rho\xi\}$ is equivalent to $\rho\xi \pmod{1}$.

The trajectory for ξ_n from $n = 0$ to $n = 20$ is computed as follows:

Table 4.2: Trajectory of $\xi_n = \{1.366 \times \xi_{n-1}\}$ for $n = 0$ to 20

n	Computation	ξ_n value
0	—	0.2000
1	$\{1.366 \times 0.2000\} = \{0.2732\}$	0.2732
2	$\{1.366 \times 0.2732\} \approx \{0.3734\}$	0.3734
3	$\{1.366 \times 0.3734\} \approx \{0.5103\}$	0.5103
4	$\{1.366 \times 0.5103\} \approx \{0.6971\}$	0.6971
5	$\{1.366 \times 0.6971\} \approx \{0.9523\}$	0.9523
6	$\{1.366 \times 0.9523\} \approx \{1.3009\}$	0.3009
7	$\{1.366 \times 0.3009\} \approx \{0.4110\}$	0.4110
8	$\{1.366 \times 0.4110\} \approx \{0.5614\}$	0.5614
9	$\{1.366 \times 0.5614\} \approx \{0.7669\}$	0.7669
10	$\{1.366 \times 0.7669\} \approx \{1.0476\}$	0.0476
11	$\{1.366 \times 0.0476\} \approx \{0.0650\}$	0.0650
12	$\{1.366 \times 0.0650\} \approx \{0.0888\}$	0.0888
13	$\{1.366 \times 0.0888\} \approx \{0.1213\}$	0.1213
14	$\{1.366 \times 0.1213\} \approx \{0.1657\}$	0.1657
15	$\{1.366 \times 0.1657\} \approx \{0.2263\}$	0.2263
16	$\{1.366 \times 0.2263\} \approx \{0.3091\}$	0.3091
17	$\{1.366 \times 0.3091\} \approx \{0.4222\}$	0.4222
18	$\{1.366 \times 0.4222\} \approx \{0.5767\}$	0.5767
19	$\{1.366 \times 0.5767\} \approx \{0.7878\}$	0.7878
20	$\{1.366 \times 0.7878\} \approx \{1.0761\}$	0.0761

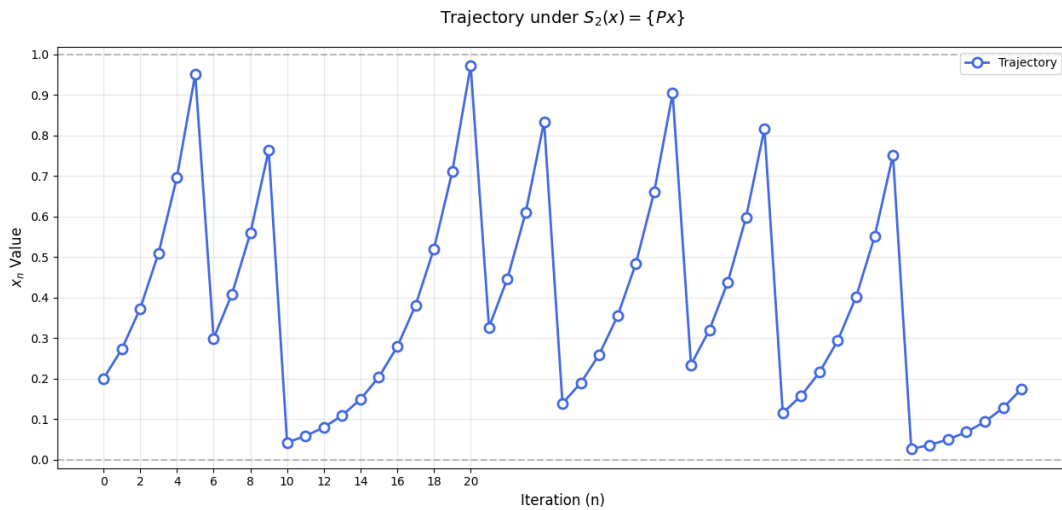


Figure 4.4: Trajectory under $\mathcal{S}_2(\xi) = \{\rho\xi\}$ for $\rho = \frac{1}{2}(\sqrt{3} + 1)$ and $\xi_0 = 0.2$.

Figure 4.4 displays the orbit of the point $\xi_0 = 0.2$ under the map $\mathcal{S}_2(\xi) = \{\rho\xi\}$, where $\rho = \frac{1}{2}(\sqrt{3} + 1) \approx 1.366$. The graph traces the values of ξ_n for $n = 0$ to 20, illustrating the dynamical behavior of the system. As the map is driven by an irrational multiplier, the orbit does not repeat or settle into a fixed cycle. Instead, it exhibits a quasi-periodic pattern with rises and sharp resets due to the modulo operation. These reset points correspond to crossings of the unit interval threshold, which is a key structural feature of irrational rotations.

4.2.2 Perron Operator for $\mathcal{S}_2(\xi) = \{\rho\xi\}$

Consider the dynamical system defined by

$$\mathcal{S}_2(\xi) = \{\rho\xi\}, \quad \text{where } \rho = \frac{1 + \sqrt{3}}{2}.$$

This transformation corresponds to the fractional part of $\rho\xi$, and can be expressed piecewise as:

$$\mathcal{S}_2(\xi) = \begin{cases} \rho\xi, & \xi \in \left[0, \frac{1}{\rho}\right), \\ \rho\xi - 1, & \xi \in \left[\frac{1}{\rho}, 1\right). \end{cases}$$

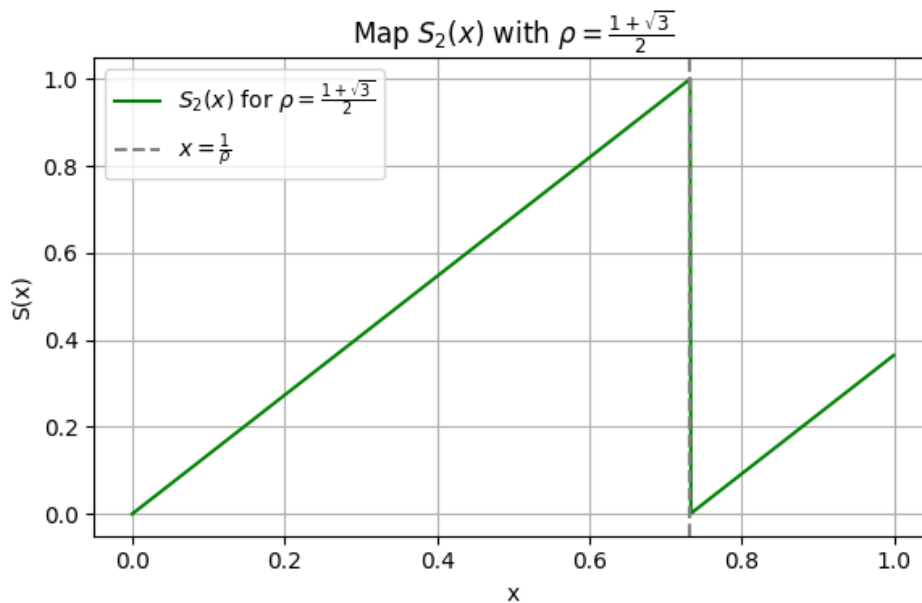


Figure 4.5: Graph of the transformation $\mathcal{S}_2(\xi) = \{\rho\xi\}$ with $\rho = \frac{1+\sqrt{3}}{2}$. The dashed line marks the discontinuity at $\xi = \frac{1}{\rho}$.

Now compute the associated Perron operator using the definition

$$P\psi(\xi) = \frac{d}{dx} \int_{\mathcal{S}_2^{-1}([0,\xi])} \psi(u) du.$$

Case 1: $\xi \in \left[0, \frac{1}{\rho}\right)$

For small values of ξ , the preimage of the interval $[0, \xi]$ includes contributions from both branches of the map

$$\mathcal{S}_2^{-1}([0, \xi]) = \left[0, \frac{\xi}{\rho}\right] \cup \left[\frac{1}{\rho}, \frac{1+\xi}{\rho}\right].$$

Differentiating the integrals over these intervals yields

$$P\psi(\xi) = \frac{1}{\rho} \left[\psi\left(\frac{\xi}{\rho}\right) + \psi\left(\frac{1+\xi}{\rho}\right) \right].$$

Case 2: $\xi \in \left[\frac{1}{\rho}, 1\right)$

For larger values of ξ , the upper bound of the second preimage segment exceeds the domain, and thus contributes nothing to the derivative

$$\mathcal{S}_2^{-1}([0, \xi]) = \left[0, \frac{\xi}{\rho}\right],$$

and hence

$$P\psi(\xi) = \frac{1}{\rho} \psi\left(\frac{\xi}{\rho}\right).$$

Combining both cases, the Perron operator for \mathcal{S}_2 is given by,

$$P\psi(\xi) = \begin{cases} \frac{1}{\rho} \left[\psi\left(\frac{\xi}{\rho}\right) + \psi\left(\frac{1+\xi}{\rho}\right) \right], & \xi \in \left[0, \frac{1}{\rho}\right), \\ \frac{1}{\rho} \psi\left(\frac{\xi}{\rho}\right), & \xi \in \left[\frac{1}{\rho}, 1\right). \end{cases}$$

4.2.3 Is the Lebesgue Measure Invariant?

To test whether the Lebesgue measure is invariant under \mathcal{S}_2 by checking whether the constant function $\psi(\xi) = 1$ satisfies $P\psi(\xi) = 1$

Case 1: $\xi < \frac{1}{\rho}$

$$P\psi(\xi) = \frac{1}{\rho}(1+1) = \frac{2}{\rho} > 1$$

Case 2: $\xi \geq \frac{1}{\rho}$

$$P\psi(\xi) = \frac{1}{\rho} \cdot 1 = \frac{1}{\rho} < 1$$

Since

$$P\psi(\xi) \neq 1 \quad \Rightarrow \quad \text{the constant density is not invariant,}$$

It is conclude that the Lebesgue measure is not preserved by the transformation \mathcal{S}_2 .

4.2.4 Frequency Analysis of $\mathcal{S}_2(\xi) = \{\rho\xi\}$

For the irrational rotation $\mathcal{S}_2(\xi) = \{\rho\xi\}$ where $\rho = \frac{1}{2}(\sqrt{3} + 1)$,

Divide $[0, 1)$ into $m = 20$ equal subintervals

$$[0, 1) = \bigcup_{i=1}^{20} \left[\frac{i-1}{20}, \frac{i}{20} \right)$$

Take initial condition $\xi_0 = \frac{\pi}{10} \approx 0.314$

Compute trajectory for $n = 20000$ iterations

$$\xi_0, \mathcal{S}_2(\xi_0), \mathcal{S}_2^2(\xi_0), \dots, \mathcal{S}_2^{5000}(\xi_0)$$

Calculate visit frequencies

$$\psi_i = \frac{1}{20000} \times \# \left\{ 1 \leq j \leq 20000 \mid \mathcal{S}_2^j(\xi_0) \in \left[\frac{i-1}{20}, \frac{i}{20} \right) \right\}$$

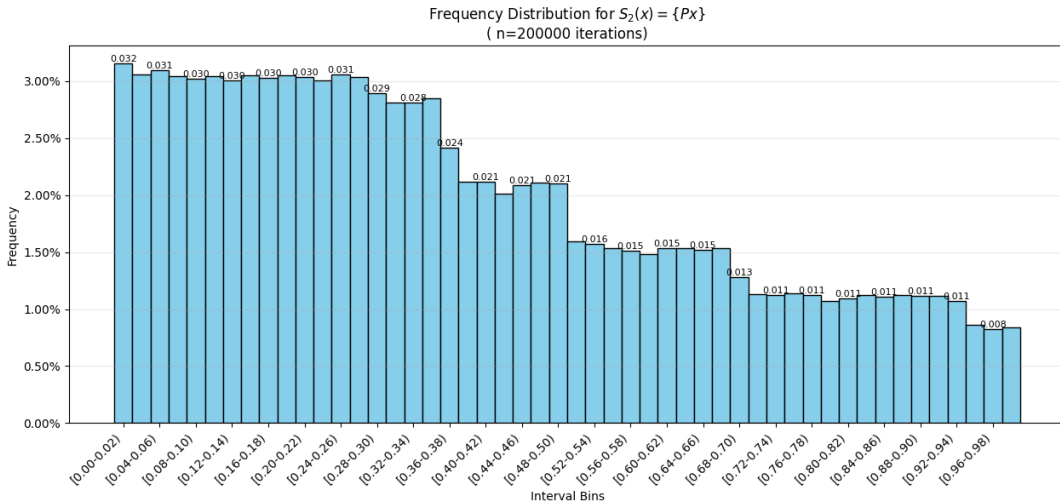


Figure 4.6: Frequency distribution for $\mathcal{S}_2(\xi) = \{\rho\xi\}$, $\rho = \frac{1}{2}(\sqrt{3} + 1)$, with $\xi_0 = \frac{\pi}{10}$ and 20000 iterations.

Figure 4.6 shows the empirical frequency distribution of the iterates of the initial point $\xi_0 = \frac{\pi}{10} \approx 0.314$ under the map $\mathcal{S}_2(\xi) = \{\rho\xi\}$, where $\rho = \frac{1+\sqrt{3}}{2}$. The unit interval $[0, 1)$ is divided into 50 equal-width bins, and the number of visits to each bin is recorded over 20,000 iterations. The resulting histogram reveals a clearly non-uniform distribution, with elevated frequencies in the lower portion of the interval and noticeably diminished frequencies in the upper range.

This observed distribution supports the conclusion that the invariant density for \mathcal{S}_2 is not uniform. However, unlike the case of the golden ratio map where the invariant density is piecewise constant, the numerical evidence here suggests a smoothly varying density. The histogram provides a visual approximation of this structure, indicating that the invariant measure is concentrated more heavily in the subinterval $[0, \frac{1}{\rho})$, but without

a sharp discontinuity in density across the domain. This aligns with the numerically estimated invariant density obtained via long-orbit interpolation.

4.2.5 Estimate Invariant Density for $\mathcal{S}_2(\xi)$

To investigate the statistical behavior of the dynamical system $\mathcal{S}_2(\xi) = \{\rho\xi\}$, where $\rho = \frac{1+\sqrt{3}}{2}$, we estimate the invariant density numerically by constructing the frequency histogram shown in Figure 4.6. This is achieved by iterating the map \mathcal{S}_2 over 10^5 steps, starting from an irrational seed $\xi_0 \in [0, 1)$, and recording the frequency of visits to each subinterval of a uniform partition of the unit interval. The resulting empirical distribution provides a numerical approximation to the invariant measure of the system.

The estimated density, depicted in Figure 4.7, is smooth and continuously varying across the interval. This contrasts sharply with the behavior observed in some special irrational systems, where piecewise constant densities arise from underlying algebraic identities. In particular, there is no indication that the density for \mathcal{S}_2 has discontinuous segments; instead, it appears to change gradually throughout the interval, reflecting the subtler arithmetic properties of ρ .

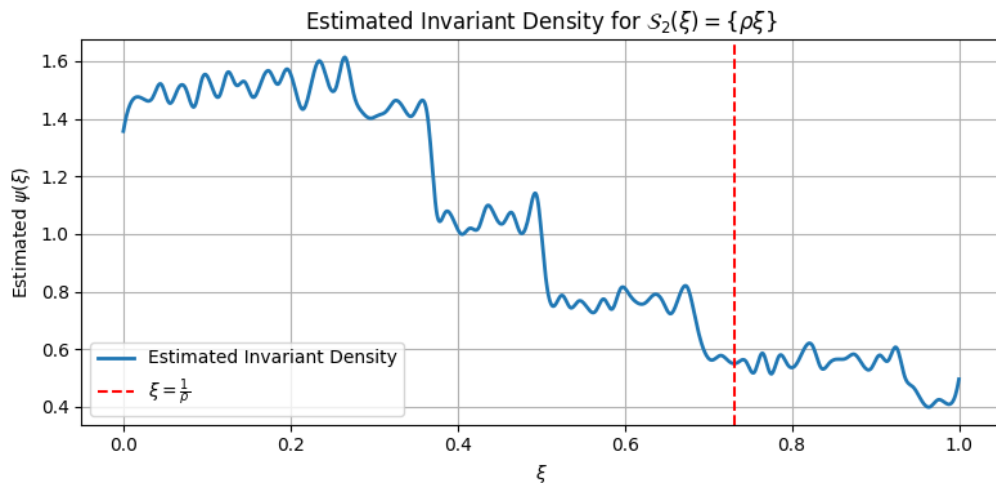


Figure 4.7: Estimated invariant density for the map $\mathcal{S}_2(\xi) = \{\rho\xi\}$, with $\rho = \frac{1+\sqrt{3}}{2}$.

4.2.6 Comparison with the Golden Ratio

Figure 4.8 illustrates a direct comparison between the invariant densities of $\mathcal{S}_2(\xi) = \{\rho\xi\}$, where $\rho = \frac{1+\sqrt{3}}{2}$, and the golden ratio map $\mathcal{S}_1(\xi) = \{G\xi\}$, where $G = \frac{1+\sqrt{5}}{2}$. The golden ratio system is known to admit a piecewise constant invariant density due to the algebraic identity $G^2 = G+1$, which simplifies the Perron equation and allows for an exact analytical solution.

In contrast, the map \mathcal{S}_2 yields a numerically estimated density that varies smoothly, suggesting the absence of a closed-form solution in simple piecewise terms. This behav-

ior is typical of irrational rotations where the multiplier does not satisfy a convenient quadratic equation, resulting in a more complex and gradually shifting invariant measure.

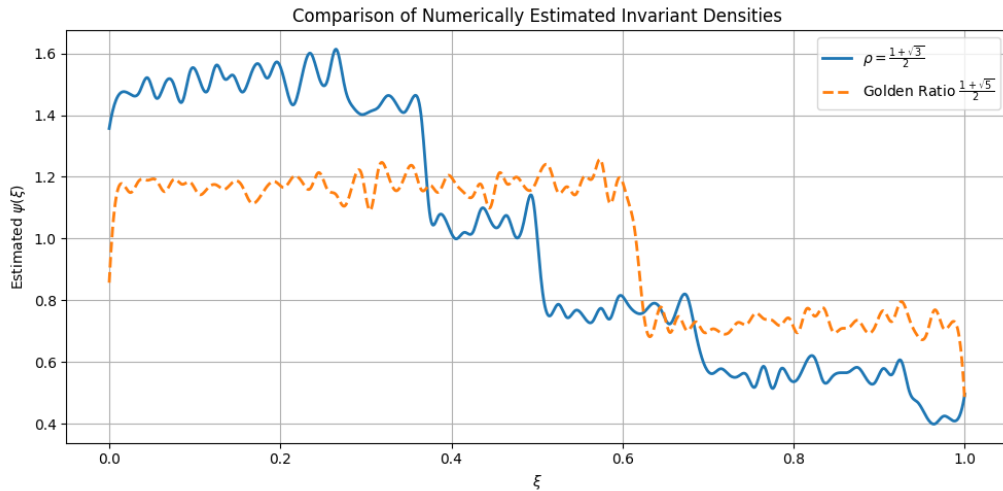


Figure 4.8: Estimated invariant densities for the maps $\mathcal{S}_2(\xi) = \{\rho\xi\}$ with $\rho = \frac{1+\sqrt{3}}{2}$ and $\mathcal{S}_1(\xi) = \{G\xi\}$ with the golden ratio $G = \frac{1+\sqrt{5}}{2}$

Thus, while both transformations are examples of irrational dynamical systems of the form $\{\rho\xi\}$, their invariant densities differ markedly depending on the arithmetic nature of the multiplier ρ . The golden ratio stands out as an exceptional case where algebraic properties yield a tractable, piecewise constant invariant density. In contrast, more general irrational constants, such as $\rho = \frac{1+\sqrt{3}}{2}$, lead to invariant densities that must be approximated numerically and reveal a richer, more nuanced structure.

4.3 Analysis of $\mathcal{S}_3(\xi) = \{\rho\xi\}$

4.3.1 Trajectory under $\mathcal{S}_3(\xi) = \{\rho\xi\}$

Analyzing the population trajectory for the map $\mathcal{S}_3(\xi) = \{\rho\xi\}$, where $\rho = \frac{1}{2}(\sqrt{7} + 1) \approx 1.8229$, and the initial state $\xi_0 = 0.2$. The fractional part $\{\rho\xi\}$ is equivalent to $\rho\xi \pmod{1}$.

The trajectory for ξ_n from $n = 0$ to $n = 20$ is computed as follows

Table 4.3: Trajectory of $\xi_n = \{1.8229 \times \xi_{n-1}\}$ for $n = 0$ to 20

n	Computation	ξ_n value
0	—	0.2000
1	$\{1.8229 \times 0.2000\} = \{0.3646\}$	0.3646
2	$\{1.8229 \times 0.3646\} \approx \{0.6646\}$	0.6646
3	$\{1.8229 \times 0.6646\} \approx \{1.2116\}$	0.2116
4	$\{1.8229 \times 0.2116\} \approx \{0.3858\}$	0.3858
5	$\{1.8229 \times 0.3858\} \approx \{0.7033\}$	0.7033
6	$\{1.8229 \times 0.7033\} \approx \{1.2821\}$	0.2821
7	$\{1.8229 \times 0.2821\} \approx \{0.5143\}$	0.5143
8	$\{1.8229 \times 0.5143\} \approx \{0.9375\}$	0.9375
9	$\{1.8229 \times 0.9375\} \approx \{1.7090\}$	0.7090
10	$\{1.8229 \times 0.7090\} \approx \{1.2926\}$	0.2926
11	$\{1.8229 \times 0.2926\} \approx \{0.5334\}$	0.5334
12	$\{1.8229 \times 0.5334\} \approx \{0.9724\}$	0.9724
13	$\{1.8229 \times 0.9724\} \approx \{1.7729\}$	0.7729
14	$\{1.8229 \times 0.7729\} \approx \{1.4090\}$	0.4090
15	$\{1.8229 \times 0.4090\} \approx \{0.7456\}$	0.7456
16	$\{1.8229 \times 0.7456\} \approx \{1.3594\}$	0.3594
17	$\{1.8229 \times 0.3594\} \approx \{0.6551\}$	0.6551
18	$\{1.8229 \times 0.6551\} \approx \{1.1942\}$	0.1942
19	$\{1.8229 \times 0.1942\} \approx \{0.3540\}$	0.3540
20	$\{1.8229 \times 0.3540\} \approx \{0.6453\}$	0.6453

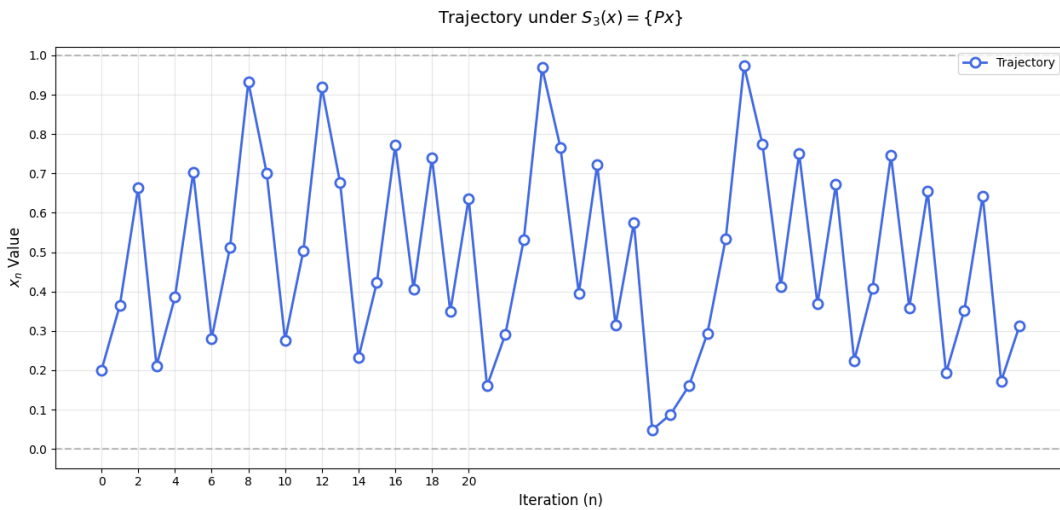


Figure 4.9: Trajectory under $\mathcal{S}_3(\xi) = \{\rho\xi\}$, with $\rho = \frac{1+\sqrt{7}}{2}$ and $\xi_0 = 0.2$.

Figure 4.9 illustrates the trajectory of the orbit starting at $\xi_0 = 0.2$ under the transformation $\mathcal{S}_3(\xi) = \{\rho\xi\}$, where $\rho = \frac{1+\sqrt{7}}{2}$. The plotted sequence ξ_n for $n = 0$ to 20 displays a complex and seemingly irregular pattern typical of irrational rotations. Although the values remain confined to the unit interval, the orbit exhibits no signs of convergence or periodicity. Instead, it moves through the space with moderate oscillations, reflecting the quasiperiodic behavior and sensitive dependence on the irrational parameter ρ .

4.3.2 Perron Operator for $\mathcal{S}_3(\xi) = \{\rho\xi\}$

Consider the transformation

$$\mathcal{S}_3(\xi) = \{\rho\xi\}, \quad \text{where } \rho = \frac{1+\sqrt{7}}{2}.$$

This map corresponds to the fractional part of $\rho\xi$ and is defined piecewise as

$$\mathcal{S}_3(\xi) = \begin{cases} \rho\xi, & \text{if } \xi \in \left[0, \frac{1}{\rho}\right), \\ \rho\xi - 1, & \text{if } \xi \in \left[\frac{1}{\rho}, 1\right). \end{cases}$$

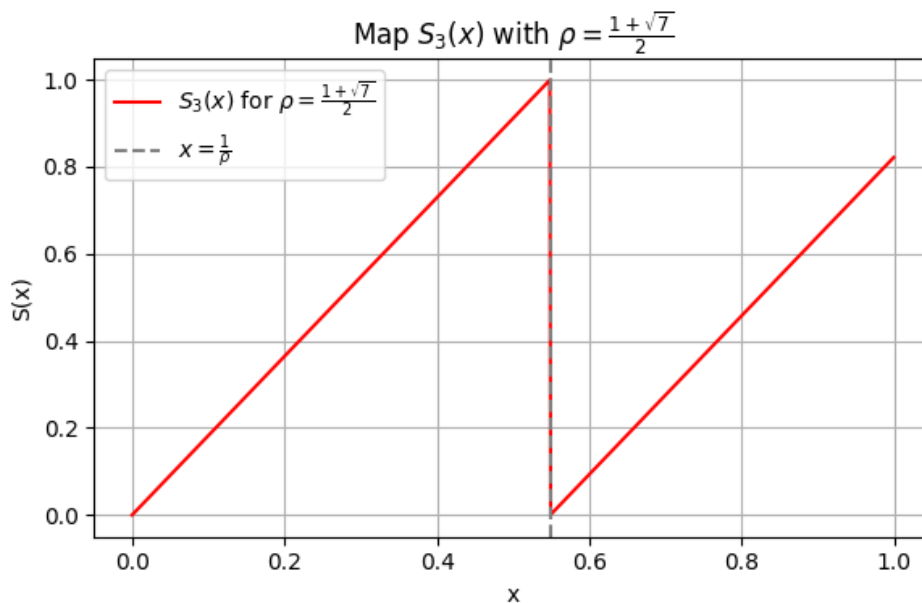


Figure 4.10: Graph of the transformation $\mathcal{S}_3(\xi) = \{\rho\xi\}$ with $\rho = \frac{1+\sqrt{7}}{2}$. The dashed line marks the discontinuity at $\xi = \frac{1}{\rho}$.

The associated Perron operator is defined by

$$P\psi(\xi) = \frac{d}{dx} \int_{\mathcal{S}_3^{-1}([0,\xi])} \psi(u) du.$$

Case 1: $\xi \in \left[0, \frac{1}{\rho}\right)$

Analyze the preimages from both branches of \mathcal{S}_3

- From the first branch: $\rho u \in [0, \xi] \Rightarrow u \in \left[0, \frac{\xi}{\rho}\right]$
- From the second branch: $\rho u - 1 \in [0, \xi] \Rightarrow u \in \left[\frac{1}{\rho}, \frac{1+\xi}{\rho}\right]$

Thus, the preimage is

$$\mathcal{S}_3^{-1}([0, \xi]) = \left[0, \frac{\xi}{\rho}\right] \cup \left[\frac{1}{\rho}, \frac{1+\xi}{\rho}\right].$$

Differentiating the total integral gives

$$P\psi(\xi) = \frac{1}{\rho}\psi\left(\frac{\xi}{\rho}\right) + \frac{1}{\rho}\psi\left(\frac{1+\xi}{\rho}\right), \quad \text{for } \xi \in \left[0, \frac{1}{\rho}\right).$$

Case 2: $\xi \in \left[\frac{1}{\rho}, 1\right)$

In this case, the second branch overshoots the domain

$$\frac{1+\xi}{\rho} > 1 \Rightarrow \text{second branch contributes nothing.}$$

Hence

$$\mathcal{S}_3^{-1}([0, \xi]) = \left[0, \frac{\xi}{\rho}\right], \quad \Rightarrow P\psi(\xi) = \frac{1}{\rho}\psi\left(\frac{\xi}{\rho}\right).$$

The Perron operator is

$$P\psi(\xi) = \begin{cases} \frac{1}{\rho} \left[\psi\left(\frac{\xi}{\rho}\right) + \psi\left(\frac{1+\xi}{\rho}\right) \right], & \xi \in \left[0, \frac{1}{\rho}\right), \\ \frac{1}{\rho} \psi\left(\frac{\xi}{\rho}\right), & \xi \in \left[\frac{1}{\rho}, 1\right). \end{cases}$$

4.3.3 Is the Lebesgue Measure Invariant?

To test invariance using the constant function $\psi(\xi) = 1$.

- For $\xi < \frac{1}{\rho}$: $P\psi(\xi) = \frac{1}{\rho}(1+1) = \frac{2}{\rho} > 1$
- For $\xi \geq \frac{1}{\rho}$: $P\psi(\xi) = \frac{1}{\rho} < 1$

Therefore, the constant function is not invariant, and the Lebesgue measure is not preserved by $\mathcal{S}_3(\xi)$.

4.3.4 Frequency Analysis of $\mathcal{S}_3(\xi) = \{\rho\xi\}$

For the irrational rotation $\mathcal{S}_3(\xi) = \{\rho\xi\}$ where $\rho = \frac{1}{2}(\sqrt{7} + 1)$,

Divide $[0, 1)$ into $m = 50$ equal subintervals

$$[0, 1) = \bigcup_{i=1}^{50} \left[\frac{i-1}{50}, \frac{i}{50} \right)$$

Take initial condition $\xi_0 = \frac{\pi}{10} \approx 0.314$

Compute trajectory for $n = 20000$ iterations

$$\xi_0, \mathcal{S}_3(\xi_0), \mathcal{S}_3^2(\xi_0), \dots, \mathcal{S}_3^{20000}(\xi_0)$$

Calculate visit frequencies

$$\psi_i = \frac{1}{20000} \times \# \left\{ 1 \leq j \leq 20000 \mid \mathcal{S}_3^j(\xi_0) \in \left[\frac{i-1}{50}, \frac{i}{50} \right) \right\}$$

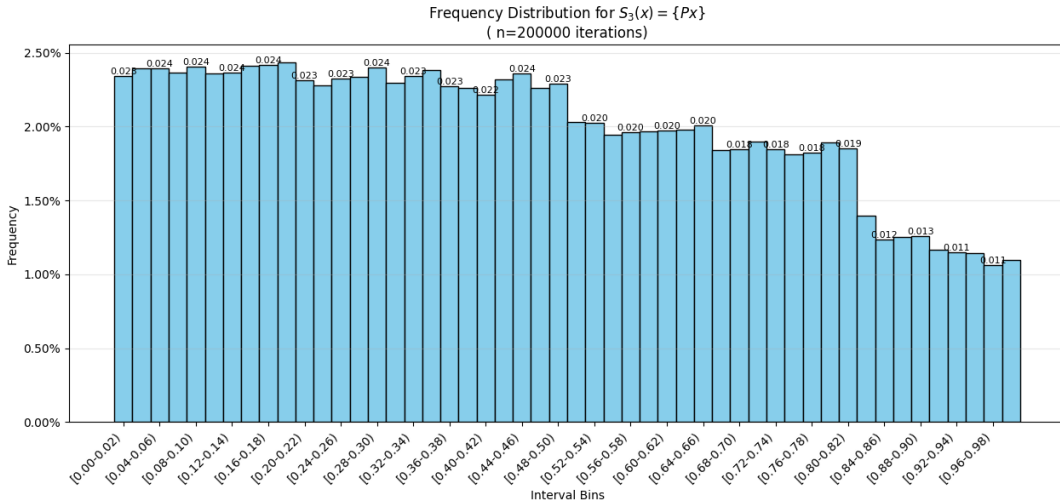


Figure 4.11: Frequency distribution for $\mathcal{S}_3(\xi) = \{\rho\xi\}$, $\rho = \frac{1+\sqrt{7}}{2}$, with $\xi_0 = \frac{\pi}{10}$ and 20000 iterations.

Figure 4.11 displays the empirical frequency histogram generated by iterating the transformation $\mathcal{S}_3(\xi) = \{\rho\xi\}$, where $\rho = \frac{1+\sqrt{7}}{2} \approx 1.823$, from the initial value $\xi_0 = \frac{\pi}{10}$. The unit interval $[0, 1)$ is divided into 50 equal-width subintervals, and the number of visits to each bin is recorded over 20,000 iterations.

The histogram reveals a clearly non-uniform distribution of orbit points, with moderate fluctuations and localized peaks throughout the interval. Unlike the uniform distribution expected under Lebesgue measure invariance, the density is skewed, with some regions visited significantly more often than others. This asymmetry suggests that the transformation stretches and folds the interval in a non-uniform way, concentrating the measure in certain subintervals over time.

Notably, the data exhibits no evidence of abrupt jumps or plateaus in the distribution, which supports the conclusion that the invariant density associated with \mathcal{S}_3 is smooth rather than piecewise constant. This observation aligns with the theoretical expectation that irrational multipliers like $\rho = \frac{1+\sqrt{7}}{2}$, generate more intricate and analytically intractable invariant measures.

4.3.5 Estimate Invariant Density for $\mathcal{S}_3(\xi)$

We now turn our attention to the dynamical system $\mathcal{S}_3(\xi) = \{\rho\xi\}$, where $\rho = \frac{1+\sqrt{7}}{2} \approx 1.823$. To examine the long-term statistical behavior of this map, we iterate \mathcal{S}_3 over 10^5 steps, starting from an irrational initial condition, and record the frequencies of orbit visits across uniformly spaced subintervals of the unit interval.

The numerically estimated invariant density is shown in Figure 4.12. The resulting function is smooth and continuous, displaying a nontrivial variation across the domain. This behavior confirms that the invariant density is not piecewise constant and reflects a more intricate underlying dynamic. Notably, the density exhibits minor fluctuations rather than sharp transitions, suggesting a gradual redistribution of mass under the action of \mathcal{S}_3 .

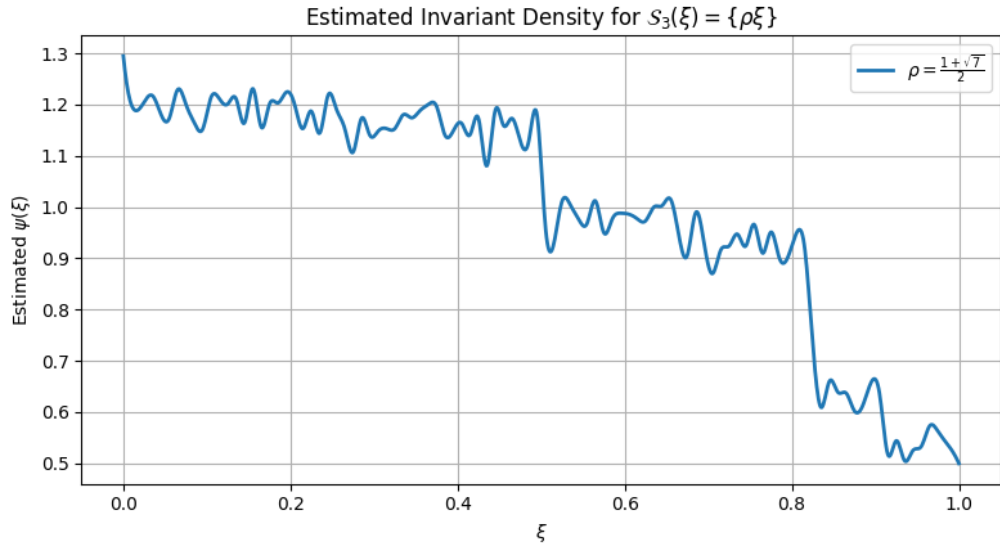


Figure 4.12: Estimated invariant density for the map $\mathcal{S}_3(\xi) = \{\rho\xi\}$, with $\rho = \frac{1+\sqrt{7}}{2}$.

4.3.6 Comparison with the Golden Ratio

To highlight the role of the arithmetic nature of ρ , we compare the invariant density for \mathcal{S}_3 with that of $\mathcal{S}_1(\xi) = \{G\xi\}$, where $G = \frac{1+\sqrt{5}}{2}$ is the golden ratio. As shown in Figure 4.13, the golden ratio system exhibits a piecewise constant invariant density with a discontinuity at $\xi = \frac{1}{G}$. This sharp structure is a direct consequence of the identity $G^2 = G + 1$, which permits an exact, algebraic solution to the associated Perron equation.

By contrast, the density for $\rho = \frac{1+\sqrt{7}}{2}$ appears much smoother and lacks any flat segments or abrupt changes. This reflects the fact that the underlying rotation does not admit any simple polynomial relation that would reduce the complexity of the system. The continuous variation of the density is consistent with the behavior observed in more general irrational rotations, where invariant measures must be approximated through numerical simulations rather than constructed analytically.

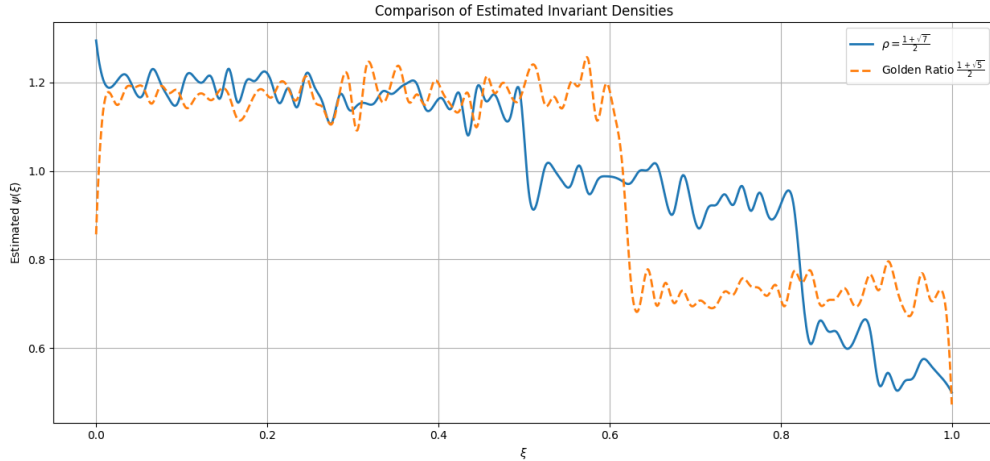


Figure 4.13: Estimated invariant densities for the maps $\mathcal{S}_3(\xi) = \{\rho\xi\}$ with $\rho = \frac{1+\sqrt{7}}{2}$ and $\mathcal{S}_1(\xi) = \{G\xi\}$ with the golden ratio $G = \frac{1+\sqrt{5}}{2}$.

This comparison illustrates a fundamental principle in ergodic theory: while the qualitative structure of the map $\{\rho\xi\}$ is preserved for any irrational ρ , the quantitative properties of the invariant measure depend sensitively on the number-theoretic nature of ρ . The golden ratio stands out as a rare example where symmetry and algebraic identity simplify the dynamics. In contrast, values like $\frac{1+\sqrt{7}}{2}$ generate invariant densities that reflect a more complex, yet deeply regular, form of dynamical behavior.

Results and Conclusions

This study examined a class of one-dimensional dynamical systems $([0, 1], B, m, \mathcal{S})$ defined by the transformation $\mathcal{S}(\xi) = \{\rho\xi\}$ on the interval $[0, 1)$, where $\rho > 1$ is irrational. Three specific maps were considered: $\mathcal{S}_1(\xi) = \{G\xi\}$, with $G = \frac{1+\sqrt{5}}{2}$; $\mathcal{S}_2(\xi) = \{\rho_2\xi\}$, with $\rho_2 = \frac{1+\sqrt{3}}{2}$; and $\mathcal{S}_3(\xi) = \{\rho_3\xi\}$, with $\rho_3 = \frac{1+\sqrt{7}}{2}$. For each system, the Perron operator was computed analytically based on the inverse images under the map. Due to the piecewise linear nature of the transformation and a discontinuity at $\xi = \frac{1}{\rho}$, each operator was expressed in two distinct cases corresponding to the subintervals $[0, \frac{1}{\rho})$ and $[\frac{1}{\rho}, 1)$.

A central result was then demonstrated, that the Lebesgue measure is not invariant under any of the three transformations. This was confirmed by evaluating the Perron operator on the constant function $\psi(\xi) = 1$, where the output differed from 1 across the domain. For instance, in the case of \mathcal{S}_1 , the operator yielded $P\psi(\xi) = \frac{2}{G}$ on $[0, \frac{1}{G})$ and $P\psi(\xi) = \frac{1}{G}$ on $[\frac{1}{G}, 1)$, violating the condition for measure invariance. Similar behavior was found in the systems defined by ρ_2 and ρ_3 .

To determine the invariant distributions, a known piecewise constant density for \mathcal{S}_1 was recalled and presented. This density satisfies $P\psi = \psi$ and integrates to one over $[0, 1)$, and is given by:

$$\psi(\xi) = \begin{cases} \frac{2G+1}{G+2}, & \xi \in [0, \frac{1}{G}), \\ \frac{G+1}{G+2}, & \xi \in [\frac{1}{G}, 1) \end{cases}$$

However, for both \mathcal{S}_2 and \mathcal{S}_3 , no consistent piecewise constant densities could be derived analytically. Attempts to solve the Perron equations with constant values on each branch did not yield a valid solution. As a result, the invariant densities for these maps could not be obtained in closed form and were instead estimated numerically.

These numerical estimates were obtained by iterating the orbit of the initial point $\xi_0 = \frac{\pi}{10}$ over 100,000 steps. The unit interval was divided into 100 subintervals, and visit frequencies were used to construct empirical histograms. In the case of \mathcal{S}_2 , the resulting invariant density was smooth and exhibited a subtle peak near the discontinuity point $\xi = \frac{1}{\rho_2}$. For \mathcal{S}_3 , the estimated density was similarly continuous but exhibited more variation across the domain, indicating a more complex redistribution of mass. In both systems, the empirical behavior provided strong evidence that the invariant densities are not piecewise constant but instead vary gradually across $[0, 1)$.

These findings demonstrate that irrational linear maps of the form $\mathcal{S}(\xi) = \{\rho\xi\}$

may redistribute mass in a non-uniform way, despite their deterministic and equidistributed trajectories. The Perron operator provides an effective tool to describe this redistribution analytically. More broadly, the work shows that linearity and irrationality do not guarantee measure preservation, and that even simple dynamical systems can exhibit rich invariant structures.

Presentation of Software Code

5.1 Numerical Algorithm for Trajectory Generation

To visualize the evolution of orbits under the irrational rotation maps $\mathcal{S}_i(\xi) = \{\rho_i\xi\}$, we employ a numerical procedure that iteratively computes and plots trajectories on the unit interval. The following general algorithm outlines the computational steps used to generate the graphs for \mathcal{S}_1 , \mathcal{S}_2 , and \mathcal{S}_3 .

Algorithm 1 Trajectory Computation under $\mathcal{S}(\xi) = \{\rho\xi\}$

- 1: **Input:** Irrational multiplier $\rho > 1$, initial point $\xi_0 \in [0, 1)$, number of iterations N
 - 2: **Initialize:** Set $\xi_0 = 0.2$, define empty list `trajectory` and append ξ_0
 - 3: **for** each $n = 1$ to N **do**
 - 4: Compute $\xi_n = \rho \cdot \xi_{n-1} \bmod 1$
 - 5: Append ξ_n to `trajectory`
 - 6: **end for**
 - 7: Generate a plot of ξ_n versus n
 - 8: Add horizontal reference lines at $y = 0$ and $y = 1$
 - 9: Label axes and format plot appearance (title, grid, legend)
 - 10: Save the plot as a high-resolution image
-

This procedure was implemented in Python using NumPy and Matplotlib. For each transformation, the multiplier ρ takes the values:

- $\rho_1 = \frac{1+\sqrt{5}}{2}$ (Golden Ratio),
- $\rho_2 = \frac{1+\sqrt{3}}{2}$,
- $\rho_3 = \frac{1+\sqrt{7}}{2}$.

Each corresponding graph visualizes how the orbit of an initial point evolves over time under the irrational rotation, allowing for qualitative comparisons of quasiperiodic behavior across different irrational parameters.

5.2 Algorithm for Plotting the Transformation $\mathcal{S}(\xi) = \{\rho\xi\}$

This algorithm computes and plots the piecewise linear maps $\mathcal{S}_i(\xi) = \{\rho_i\xi\}$ for irrational values $\rho_i = \frac{1+\sqrt{d}}{2}$ where $d = 5, 3, 7$. Each map is defined piecewise as:

$$\mathcal{S}(\xi) = \begin{cases} \rho\xi, & \xi \in [0, \frac{1}{\rho}) \\ \rho\xi - 1, & \xi \in [\frac{1}{\rho}, 1) \end{cases}$$

Algorithm 2 Plotting the Graphs of Piecewise Maps $\mathcal{S}(\xi) = \{\rho\xi\}$

1: **Input:** Irrational values $\rho_1 = \frac{1+\sqrt{5}}{2}$, $\rho_2 = \frac{1+\sqrt{3}}{2}$, $\rho_3 = \frac{1+\sqrt{7}}{2}$

2: Define the function:

$$\mathcal{S}_\rho(\xi) = \begin{cases} \rho \cdot \xi, & \text{if } \xi < \frac{1}{\rho} \\ \rho \cdot \xi - 1, & \text{otherwise} \end{cases}$$

3: Discretize the domain: generate a fine partition $\xi \in [0, 1)$

4: **for** each ρ_i in $\{\rho_1, \rho_2, \rho_3\}$ **do**

5: Compute $\mathcal{S}_i(\xi) = \mathcal{S}_{\rho_i}(\xi)$ over the domain

6: Plot the function $\mathcal{S}_i(\xi)$ along with a dashed line at $\xi = 1/\rho_i$ to show the discontinuity

7: **end for**

8: Display each graph with labeled axes, title, legend, and grid lines

These plots provide insight into the structure and discontinuities of the transformations. The dashed vertical lines at $\xi = \frac{1}{\rho}$ highlight the change in definition of each map, revealing the partition over which the Perron operator must be evaluated.

5.3 Algorithm for Frequency Histogram Computation

To investigate the statistical behavior of irrational rotation maps $\mathcal{S}_i(\xi) = \{\rho_i\xi\}$, this algorithm computes the empirical frequency distribution of orbit points over a fixed number of iterations. The unit interval $[0, 1)$ is divided into equal-length subintervals (bins), and the frequency of trajectory visits in each bin is recorded and visualized as a histogram.

Algorithm 3 Empirical Frequency Histogram for $\mathcal{S}(\xi) = \{\rho\xi\}$

- 1: **Input:** Irrational multiplier $\rho > 1$, initial point $\xi_0 \in [0, 1)$, number of iterations n , number of bins m
 - 2: **Initialize:** Set empty list `trajectory`; assign $\xi \leftarrow \xi_0$
 - 3: **for** each iteration $i = 1$ to n **do**
 - 4: Update $\xi \leftarrow \{\rho\xi\} = (\rho \cdot \xi) \bmod 1$
 - 5: Append ξ to `trajectory`
 - 6: **end for**
 - 7: Divide the interval $[0, 1)$ into m equal subintervals (bins)
 - 8: Count how many trajectory points fall into each bin to get histogram frequencies
 - 9: Normalize frequencies by dividing by total number of iterations n
 - 10: Plot the histogram as a bar chart with appropriate axis labels and bin indicators
-

This procedure was executed in Python using NumPy and Matplotlib, and applied separately for the following irrational multipliers:

- $\rho_1 = \frac{1+\sqrt{5}}{2}$ (Golden Ratio),
- $\rho_2 = \frac{1+\sqrt{3}}{2}$,
- $\rho_3 = \frac{1+\sqrt{7}}{2}$.

For each map, the resulting histogram captures how the orbit populates subintervals of $[0, 1)$, revealing deviations from uniformity and helping visualize the shape of invariant densities.

5.4 Algorithm for Invariant Density Estimation

This algorithm refines the empirical histogram of a dynamical system $\mathcal{S}(\xi) = \{\rho\xi\}$ to produce a smooth approximation of the invariant density. The process combines orbit simulation, histogram construction, and function interpolation.

Algorithm 4 Smooth Invariant Density Estimation for $\mathcal{S}(\xi) = \{\rho\xi\}$

- 1: **Input:** Irrational parameter $\rho > 1$, initial value $\xi_0 \in [0, 1)$, number of iterations N , number of bins m
 - 2: **Define:** Transformation $\mathcal{S}(\xi) = (\rho \cdot \xi) \bmod 1$
 - 3: **Initialize:** Set ξ_0 and create array `orbit` of length N
 - 4: **for** each $i = 1$ to $N - 1$ **do**
 - 5: $\xi_i \leftarrow \mathcal{S}(\xi_{i-1})$
 - 6: **end for**
 - 7: Construct a histogram from $\{\xi_i\}$ with m bins over interval $[0, 1)$
 - 8: Compute bin centers x_i and normalized histogram values ψ_i
 - 9: **Interpolate:** Fit a cubic spline $\psi_{\text{smooth}}(\xi)$ through (x_i, ψ_i)
 - 10: Evaluate ψ_{smooth} on a dense grid over $[0, 1)$
 - 11: **Output:** Smoothed approximation $\psi_{\text{smooth}}(\xi)$ of the invariant density
-

This algorithm was applied to the following two transformations:

- $\mathcal{S}_2(\xi) = \{\rho_2\xi\}$, with $\rho_2 = \frac{1+\sqrt{3}}{2}$,
- $\mathcal{S}_3(\xi) = \{\rho_3\xi\}$, with $\rho_3 = \frac{1+\sqrt{7}}{2}$.

The smoothed densities reveal subtle structural patterns not immediately visible in the raw histogram, enabling visual comparison with the known piecewise constant density in the golden ratio case.

5.5 Algorithm for Comparative Density Estimation of Irrational Maps

This algorithm computes and compares the numerically estimated invariant densities of two irrational rotation maps. One uses the golden ratio $G = \frac{1+\sqrt{5}}{2}$ as the multiplier, and the other uses a chosen irrational constant $\rho \in \left\{ \frac{1+\sqrt{3}}{2}, \frac{1+\sqrt{7}}{2} \right\}$. A common initial condition and number of iterations are used to generate orbits, construct histograms, and then apply cubic spline interpolation for smoothing.

Algorithm 5 Comparison of Estimated Invariant Densities for Two Irrational Maps

- 1: **Input:** Irrational constants $\rho > 1$, golden ratio $G = \frac{1+\sqrt{5}}{2}$, initial value $\xi_0 \in [0, 1)$, number of iterations N , number of bins m
 - 2: **Define:** Map $\mathcal{S}(x, \gamma) = (\gamma \cdot x) \bmod 1$, where $\gamma \in \{\rho, G\}$
 - 3: **Generate Orbits:**
 - 4: **for** each $i = 1$ to $N - 1$ **do**
 - 5: $\xi_i^{(\rho)} \leftarrow \mathcal{S}(\xi_{i-1}^{(\rho)}, \rho)$
 - 6: $\xi_i^{(G)} \leftarrow \mathcal{S}(\xi_{i-1}^{(G)}, G)$
 - 7: **end for**
 - 8: **Construct Histograms:**
 - Use m equal-width bins on $[0, 1)$ to compute normalized histograms for both orbits
 - Compute bin centers x_i , and histogram heights $\psi_i^{(\rho)}, \psi_i^{(G)}$
 - 9: **Smooth Histograms:** Fit cubic splines through histogram data to obtain smooth functions
$$\psi_{\text{smooth}}^{(\rho)}(\xi), \quad \psi_{\text{smooth}}^{(G)}(\xi)$$
 - 10: **Output:** Smooth density curves $\psi^{(\rho)}(\xi)$ and $\psi^{(G)}(\xi)$ for comparison
-

The output consists of two curves plotted over the interval $[0, 1)$. The comparison illustrates how the invariant measure associated with the irrational constant ρ differs from that of the golden ratio, both in shape and smoothness. The algorithm was executed for:

- $\rho = \frac{1+\sqrt{3}}{2}$ vs. $G = \frac{1+\sqrt{5}}{2}$
- $\rho = \frac{1+\sqrt{7}}{2}$ vs. $G = \frac{1+\sqrt{5}}{2}$

with results confirming nontrivial deviations in invariant densities.

Bibliography

- [1] Lasota, A.; Yorke, J. A. Exact dynamical systems and the Frobenius-Perron operator. *Transactions of the American Mathematical Society* **1982**, 273(1), 375–384.
- [2] Sahai, T. Dynamical systems theory and algorithms for NP-hard problems. In: *Advances in Dynamics, Optimization and Computation*. Springer: Berlin, 2020; pp. 183–206.
- [3] Hasselblatt, B.; Katok, A. *A First Course in Dynamics*. Cambridge University Press: Cambridge, 2003.
- [4] [Jonas Siaulyš Lecture notes of Dynamic Systems]
- [5] Ishikawa, I.; et al. Metric on nonlinear dynamical systems with Perron-Frobenius operators. *Advances in Neural Information Processing Systems* **2018**, 31.
- [6] Arnold, V. I.; Avez, A. *Ergodic Problems of Classical Mechanics*. Benjamin: New York, 1968.
- [7] Petersen, K. *Ergodic Theory*. Cambridge University Press: Cambridge, 1989.
- [8] Mackey, M. C.; Tyran-Kamińska, M. Density evolution under delayed dynamics. *Chaos* **2021**, 31(4), 043120.
- [9] Lasota, A.; Mackey, M. C. *Chaos, Fractals, and Noise: Stochastic Aspects of Dynamics*, 2nd ed.; Springer: New York, 1994.
- [10] Einsiedler, M.; Ward, T. *Ergodic Theory with a View Towards Number Theory*. Springer: London, 2011.
- [11] Kuipers, L.; Niederreiter, H. *Uniform Distribution of Sequences*. Wiley: New York, 1974.
- [12] Hmissi, M. Koopman and Perron-Frobenius operators of random systems. *ESAIM: Proceedings* **2014**, 46, 132–145.
- [13] Klus, S.; et al. Approximation of Perron-Frobenius and Koopman operators. *arXiv preprint* **2015**, arXiv:1512.05997.

- [14] Chiba, H.; et al. Generalized eigenvalues of the Perron-Frobenius operators. *SIAM Journal on Applied Dynamical Systems* **2023**, *22*(4), 2825–2855.
- [15] Froyland, G.; Stancevic, O. Escape rates and Perron-Frobenius operators in open systems. *Discrete and Continuous Dynamical Systems - Series B* **2010**, *14*(2), 457–472.
- [16] Canto-Martín, F.; et al. Perron-Frobenius operators and the Klein-Gordon equation. *Journal of the European Mathematical Society* **2014**, *16*(1), 31–66.
- [17] Steuding, J. *Diophantine Analysis*. Chapman & Hall/CRC: Boca Raton, 2005.
- [18] Ikeda, M.; et al. Operators on reproducing kernel Banach spaces. *Chaos* **2022**, *32*(12), 123134.
- [19] Liu, N.; Jiang, L. Frobenius-Perron operator filter for stochastic systems. *SIAM/ASA Journal on Uncertainty Quantification* **2024**, *12*(1), 182–211.